Mon. Not. R. Astron. Soc. (2006) doi: 10.1111/j.1365-2966.2006.10876.x

# Formation and evolution of compact binaries in globular clusters – I. Binaries with white dwarfs

N. Ivanova,[1]★ C. O. Heinke,[2]† F. A. Rasio,[2] R. E. Taam,[2] K. Belczynski[3]‡ and J. Fregeau[2]

[1]*Canadian Institute for Theoretical Astrophysics, University of Toronto, 60 St George, Toronto, ON M5S 3H8, Canada*
[2]*Department of Physics & Astronomy, Northwestern University, 2145 Sheridan Road, Evanston, IL 60208, USA*
[3]*Department of Astronomy, New Mexico State University, 1320 Frenger Mall, Las Cruces, NM 88003-8001, USA*

Accepted 2006 July 26. Received 2006 June 23; in original form 2006 April 4

**ABSTRACT**

In this paper, the first of a series, we study the stellar dynamical and evolutionary processes leading to the formation of compact binaries containing white dwarfs (WDs) in dense globular clusters (GCs). We examine the processes leading to the creation of X-ray binaries such as cataclysmic variables (CVs) and AM CVn systems. Using numerical simulations, we identify the dominant formation channels and we predict the expected numbers and characteristics of detectable systems, emphasizing how the cluster sources differ from the field population. We explore the dependence of formation rates on cluster properties and we explain in particular why the distribution of CVs has only a weak dependence on cluster density. We also discuss the frequency of dwarf nova outbursts in GCs and their connection with moderately strong WD magnetic fields. We examine the rates of Type Ia supernovae (SNe Ia) via both single and double degenerate channels in clusters and we argue that those rates may contribute to the total SN Ia rate in elliptical galaxies. Considering coalescing WD binaries, we discuss possible constraints on the common envelope evolution of their progenitors and we derive theoretical expectations for gravitational wave detection by *Laser Interferometer Space Antenna* (*LISA*).

**Key words:** stellar dynamics – binaries: close – binaries: general – globular clusters: general.

## 1 INTRODUCTION

From the earliest observations of X-ray binaries in globular clusters (GCs), it has been noted that they must be very efficient sites for the production of compact binary systems (Clark 1975). The key to the overabundance of compact binaries in clusters, as compared to the field, is close stellar encounters. The processes that influence the binary population in dense stellar environments include the destruction of wide binaries ('ionization'), hardening of close binaries, physical collisions, and exchange interactions, through which low-mass companions tend to be replaced by more-massive participants in the encounter. As a result of these processes, in the dense cores of GCs, binaries are strongly depleted and their period distribution is very different from that of a field population (Ivanova et al. 2005a). This effect is stronger for binaries including a compact object, like cataclysmic variables (CVs).

The issue of the dynamical formation of CVs has been extensively discussed. Considering the CV formation via tidal captures (TCs), Bailyn, Grindlay & Garcia (1990) showed that dynamical formation of CVs is not expected because more-massive donors lead to unstable mass transfer (MT). On the other hand, Di Stefano & Rappaport (1994) predicted the existence of many CVs formed via TCs, as many as an order of magnitude more than that would be predicted by standard binary evolution, making CVs a probe of the dynamical processes in the cluster. Detection of CVs in GCs proved difficult (e.g. Shara et al. 1996), but a population was detected using the *Hubble Space Telescope* (*HST*) (Cool et al. 1995), along with a population of 'non-flickerers' (Cool et al. 1998) which are understood to be young helium white dwarfs (WDs) with carbon–oxygen (CO) WD companions (Hansen, Kalogera & Rasio 2003).

In the past few years, substantial progress has been made in optical identification of *HST* counterparts to *Chandra* X-ray sources in several GCs. Valuable information was obtained for populations of CVs, chromospherically active binaries and quiescent low-mass X-ray binaries (qLMXBs) (Grindlay et al. 2001a; Pooley et al. 2002; Edmonds et al. 2003a; Heinke et al. 2003; Bassa et al. 2004). For the first time, we can compare populations of such binaries in GCs and in the Galactic field, and infer their rates of formation and population characteristics. In particular, 22 CVs have now been identified in 47 Tuc, allowing identification of several differences between typical CVs in GCs and CVs in the Galactic field. These differences include relatively high X-ray luminosities compared to field systems

★E-mail: nata@cita.utoronto.ca
† Lindheimer Fellow.
‡Tombaugh Fellow.

© 2006 The Authors. Journal compilation © 2006 RAS

(Verbunt et al. 1997); a lack of novae, and of the steady, bright blue accretion discs signifying nova-like CVs, in GCs (Shara & Drissen 1995); relatively low frequencies of dwarf nova outbursts (DNOs), the typical identifiers of CVs in the Galactic disc (Shara et al. 1996); and a higher ratio of X-ray to optical flux than that in most field CVs (Edmonds et al. 2003b). These differences produce puzzles: the lack of novae, nova-likes, and DNO suggests very low MT rates, while the high X-ray luminosities indicate moderate MT rates. The X-ray to optical flux ratio suggests the CVs are dwarf novae, but the lack of DNO argues against this. It was suggested that CV discs in GCs are more stable due to a combination of low MT rates and moderately strong WD magnetic moments (Dobrotka, Lasota & Menou 2006). This hints that the evolutionary paths of CVs in GCs and in the field are different. Comparisons of the numbers of CVs in clusters of different central densities also support the idea that CVs are produced through dynamical interactions (Pooley et al. 2003), though there is an indication that CV production may depend more weakly on density than on the production of LMXBs containing neutron stars (NSs) (Heinke et al. 2003). Recent comparisons of colour distributions of CVs in NGC 6399, NGC 6266, and 47 Tuc with those of CVs in the field confirm the dynamical origin of cluster CVs (Pooley & Hut 2006).

This is the first of two papers where we summarize results of our studies on compact binary formation in GCs, some preliminary results of which were reported in Ivanova, Fregeau & Rasio (2005b) and Ivanova & Rasio (2004, 2005). In this paper, we focus on the formation of compact binaries with a WD, and in the second paper (Paper II) we will describe dynamical formation and evolution of binaries with an NS companion. We explore a large spectrum of GC models, where for the first time we take into account (i) the mechanism of binary formation through physical collisions using results from smoothed particle hydrodynamics (SPH), and (ii) the effect of metallicity on the formation and subsequent evolution of close binaries. In Section 2, we provide a complete review of the physical processes of formation and destruction of mass-transferring WD binaries. In Section 3, we outline the methods and assumptions. The major formation channels, and population characteristics for CVs and AM CVn systems (double WD systems where one WD experiences Roche lobe overflow) in different clusters are presented and discussed in Section 4. We conclude in the last section by addressing the connection between our results and the observations.

## 2 MASS-TRANSFERRING WHITE DWARF BINARIES IN A DENSE CLUSTER

There are several ways to destroy a primordial binary in a GC. For instance, in a dense region a soft binary will very likely be 'ionized' (destroyed) as a result of a dynamical encounter. A hard binary, in contrast, can be destroyed through a physical collision during the encounter. The probability of such an outcome increases strongly as the binary becomes harder (Fregeau et al. 2004). In addition to dynamical processes, a primordial binary can be destroyed either through an evolutionary merger or following a supernova (SN) explosion. Overall, even if a cluster initially had 100 per cent of its stars in binaries initially, the binary fraction at an age of 10–14 Gyr will typically be as low as 10 per cent (Ivanova et al. 2005a).

To understand the evolution of a primordial binary in a dense environment and the probability of a binary becoming a CV, two steps are required: (i) compare the evolutionary time-scales with the time-scale of dynamical encounters; and (ii) analyse what is the consequence of an encounter (this depends strongly on the hardness of the binary). A similar approach was also used, for example, in Davies (1997).

The time-scale for a binary to undergo a strong encounter with another single star (the collision time) can be estimated as $\tau_{\rm coll} = (n\Sigma v_\infty)^{-1}$. Here, $\Sigma$ is the cross-section for an encounter between two objects, of masses $m_i$ and $m_j$, with relative velocity at infinity $v_\infty$ and is given by

$$\Sigma = \pi d_{\rm max}^2 \left(1 + \frac{v_{\rm p}^2}{v_\infty^2}\right), \tag{1}$$

where $d_{\rm max}$ is the maximum distance of closest approach that defines a significant encounter and $v_{\rm p}^2 = 2G\,(m_i + m_j)/d_{\rm max}$ is the velocity at pericentre. Assuming that a strong encounter occurs when the distance of closest approach is a few times the binary separation $a$, $d_{\rm max} \leqslant ka$ with $k \simeq 2$, we obtain

$$\tau_{\rm coll} = 3.4 \times 10^{13}\ {\rm yr}\ k^{-2} P_{\rm d}^{-4/3} M_{\rm tot}^{-2/3} n_5^{-1} v_{10}^{-1} \times \left[1 + 913 \frac{(M_{\rm tot} + \langle M\rangle)}{k P_{\rm d}^{2/3} M_{\rm tot}^{1/3} v_{10}^2}\right]^{-1}. \tag{2}$$

Here $P_{\rm d}$ is the binary period in days, $M_{\rm tot}$ is the total binary mass in $\rm M_\odot$, $\langle M\rangle$ is the mass of an average single star in $\rm M_\odot$, $v_{10} = v_\infty/(10\ {\rm km\ s^{-1}})$ and $n_5 = n/(10^5\ {\rm pc^{-3}})$, where $n$ is the stellar number density.

The hardness of a binary system, $\eta$, is defined as

$$\eta = \frac{G m_1 m_2}{a\sigma^2 \langle m\rangle}, \tag{3}$$

where $a$ is the binary separation, $\sigma$ is the central velocity dispersion, $m_1$ and $m_2$ are the masses of the binary components, and $\langle m\rangle$ is the average mass of a single star. Binaries that have $\eta < 1$ are termed soft, and those with $\eta > 1$ are termed hard.

### 2.1 Primordial CVs and AM CVn systems

The typical formation scenario for CVs in the field (low-density environment) usually involves common envelope (CE) evolution. In Fig. 1, we show parameters of primordial non-eccentric binaries that successfully become CVs. To obtain this parameter space, we used the binary population synthesis code STARTRACK (Belczynski, Kalogera & Bulik 2002; Belczynski et al. 2005c).[1] We evolved $5 \times 10^5$ binaries considering specifically that region of primordial binaries which, according to preliminary lower-resolution runs, leads to CV formation. Our primary stars have masses between 0.5 and 10 $\rm M_\odot$, the secondaries have masses according to a flat mass ratio distribution with initial periods distributed flatly between 1 and $10^4$ d. For demonstration purposes in Fig. 1, we use initially circular orbits, because the parameters leading to different formation channels can be more clearly distinguished. For our actual cluster simulations, we use eccentric binaries; in comparison to Fig. 1, eccentric primordial binaries can have higher initial periods and still produce CVs. Progenitors of CVs with a main-sequence (MS) donor are located in the left-hand bottom corner, with $M_{\rm p} \lesssim 4\ \rm M_\odot$ and $\log P \lesssim 2.5$. In other cases, the donor star is a red giant (RG) or a (subgiant) star in the Hertzsprung gap. For primordial binaries located in a small but dense area at the left-hand middle part of Fig. 1, $\log P \sim 2.7$ and $M_{\rm p} \sim 1\ \rm M_\odot$, a CE does not occur. We note that the lifetime of a

[1] For the calculations in this study, we have used the STARTRACK code prior to the latest release (Belczynski et al. 2005c). However, the most important updates and revisions of input physics, in particular the ones important for evolution of binaries with WDs, were already incorporated in the version we have used.

© 2006 The Authors. Journal compilation © 2006 RAS, MNRAS

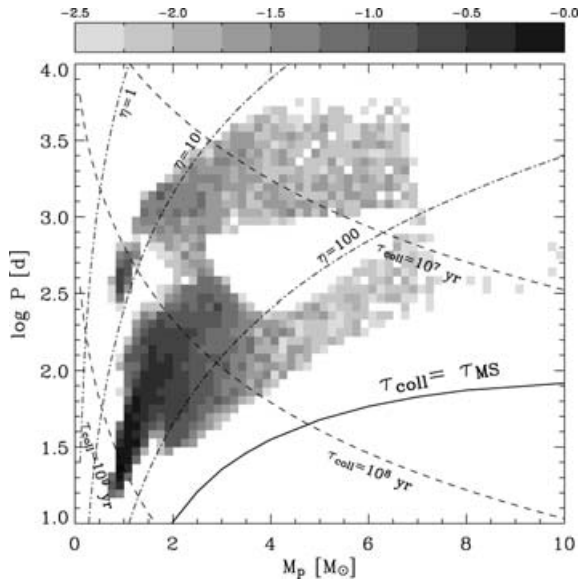


**Figure 1.** Distribution density of CV progenitors (initial masses of primary stars $M_{\rm p}$ and binary periods $P$) for non-eccentric binaries in the Galactic field, with $Z = 0.001$. The total normalization of CV progenitors is scaled to unity, the grey colour shows $\log_{10}$ of the normalized distribution density. The thick solid line indicates the binary period where the collision time of the binary is equal to the MS lifetime of the primary (using a core number density $n = 10^5$ pc$^{-3}$, a central velocity dispersion 10 km s$^{-1}$ and an average object mass of 0.5 M$_\odot$). The dash–dotted lines are lines of constant binary hardness and the dashed lines are lines of constant collision time.

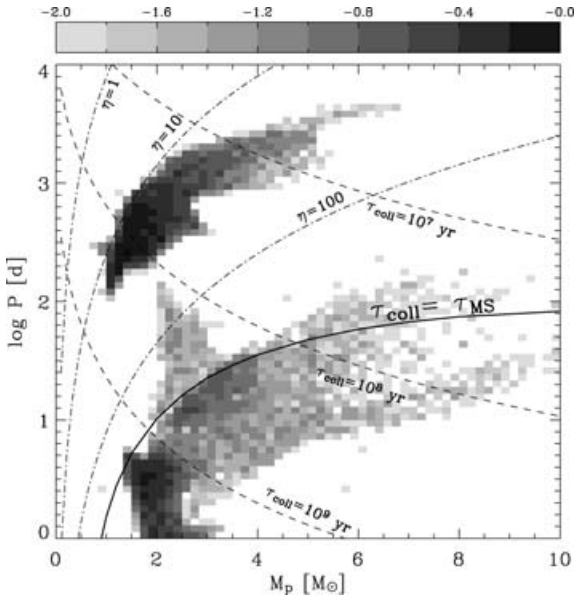


**Figure 2.** Distribution density of AM CVn progenitors (initial masses of primary stars $M_{\rm p}$ and binary periods $P$) for non-eccentric binaries in the Galactic field, $Z = 0.001$. Notation as for Fig. 1.

binary in the CV stage with an RG donor is about 1000 times shorter than in the case of an MS donor.

In the core of a GC with core density $\rho_{\rm c} \sim 10^5$ pc$^{-3}$, a binary with an initial period typical of a CV progenitor will experience a dynamical encounter before its primary leaves the MS (see Fig. 1, where all CV progenitors lie above the line indicating equality of $\tau_{\rm coll}$ and $\tau_{\rm MS}$). The unaltered primordial channel for CV formation is therefore likely to succeed only for binaries that enter the dense cluster core after their CE event; the post-CE binary is compact enough to avoid an encounter. The contribution of the primordial channel depends therefore on the time – before or after the moment of CE – when primordial CV binaries will segregate into the central dense core. In more detail, an average initial binary in the GC is $\sim 0.7$ M$_\odot$, which is significantly smaller than the pre-CE mass of a primordial CV binary (see Fig. 1). Post-CE primordial CV binaries are also heavier than typical binaries in the halo (for which the average binary mass is $\sim 0.4$ M$_\odot$). In both cases, primordial CV binaries, as heavier objects, will tend to sink towards the cluster core on the cluster half-mass relaxation time.

The situation is similar for the formation of AM CVn systems from primordial binaries (see Fig. 2). In this case, the main formation channel requires the occurrence of two CE events (see also Belczynski et al. 2005a), and the primordial binary is expected to be even wider. However, the second channel, with two stable MT stages (at the start of the RG stage of the primary, and when the secondary becomes a helium giant), is provided by relatively compact progenitor binaries. These binaries are expected to evolve in the same way in a GC as in the field.

### 2.2 Dynamical formation of CVs

A binary consisting of an MS star and a WD can be formed via several kinds of dynamical encounters: via an exchange interaction, via a TC of an MS by a WD, or via physical collisions between an RG and an MS star. A fraction of these dynamically formed MS–WD binary systems will start MT and become a CV. In this section we examine in detail the possible channels for CV creation.

The main angular momentum losses in a close MS–WD binary occur via magnetic braking (MB) and gravitational wave (GW) emission, both of which lead to orbital decay. In eccentric binaries, the binary orbital separation will be affected by tides, and the post-circularized periastron is larger than the pre-circularized periastron (unless tidal synchronization is significant). In Fig. 3, we show the maximum initial periods (at the moment of the binary formation) of a non-eccentric MS–WD binary that can start MT within 2 Gyr, and within 10 Gyr, due only to GW or only to MB [for illustrative purposes, we show time-scales for two prescriptions of MB, one is standard MB according to Rappaport et al. 1983 (hereafter RVJ), and the second is the MB based on dipole-field model according to Ivanova & Taam 2003 (hereafter IT03)]. A maximum initial period such that a binary is able to start MT without having any other encounters is only $\sim$2 d. In Fig. 4, we again show the maximum initial periods of binaries that may start MT, but now including all angular momentum losses (GW, MB and tides), and compare the cases of non-eccentric and eccentric binaries. In this figure, we also show the difference in maximum initial period between metal-poor and metal-rich GCs. In metal-poor clusters only stars with $M \lesssim 0.85$ M$_\odot$ have developed outer convective zones, allowing MB and convective tides to operate (Ivanova 2006). This effect can potentially be dramatic; for instance, among non-eccentric binaries with an MS star of 1 M$_\odot$, the range of post-exchange periods that leads to CV formation is a factor of 6 larger if the donor has $Z = 0.02$, compared to $Z = 0.001$. For eccentric binaries, this ratio is higher, as tidal circularization via radiative damping will reduce binary eccentricity (and therefore increase the periastron) more effectively than GW can shrink the binary orbit.

A circular binary is most likely to be formed via TC, where a post-capture circularization is assumed. Using the approach described in Portegies Zwart & Meinen (1993), we can estimate the post-capture

© 2006 The Authors. Journal compilation © 2006 RAS, MNRAS

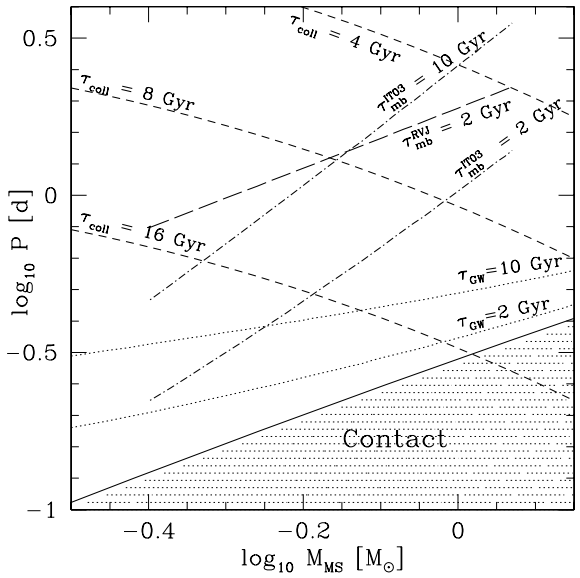


**Figure 3.** The fate of non-eccentric MS–WD binaries produced by, for example, dynamical encounters, where the primary is a WD of 0.6 $M_\odot$. $P$ is the post-encounter (or post-CE) orbital period and $M_{\rm MS}$ is the mass of an MS secondary. The short-dashed lines show the binary periods for constant collision times and the dotted lines delineate the binaries that will shrink within 2 and 10 Gyr due to GW emission. The long-dashed line indicates the upper period limit for binaries that will begin MT within 2 Gyr with the RVJ MB prescription, whereas the dash–dotted lines indicate those that will begin MT within 2 and 10 Gyr with IT03 MB. Below the solid line the binary is in contact.

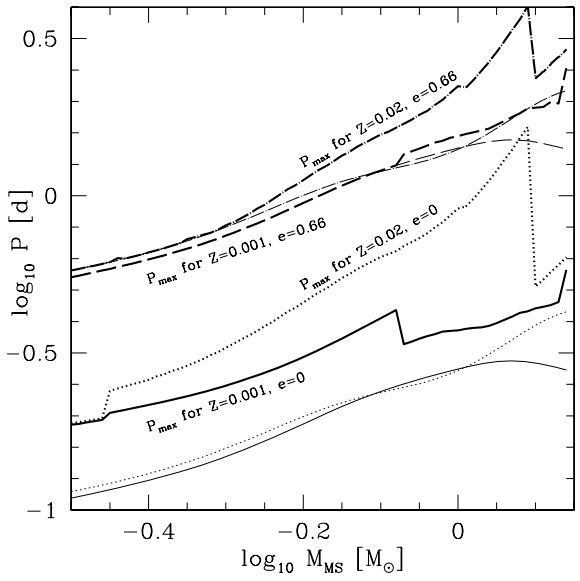


**Figure 4.** The fate of post-encounter MS–WD binaries where the primary is a WD of 0.6 $M_\odot$, for post-exchange eccentricities 0 and 0.66. $P$ is the post-encounter orbital period and $M_{\rm MS}$ is the mass of the MS secondary. The thick lines delineate the maximum periods for binaries which will begin MT within 2 Gyr. The thin lines of the same type show the period at which that binary will begin MT.

binary parameters for an MS–WD binary (see Fig. 5, where WD mass is assumed to be 0.6 $M_\odot$). The upper limit here corresponds to the closest approach at which tidal interactions are strong enough to make a bound system, and the lower limit corresponds to the closest approach at which the MS star overfills its Roche lobe by

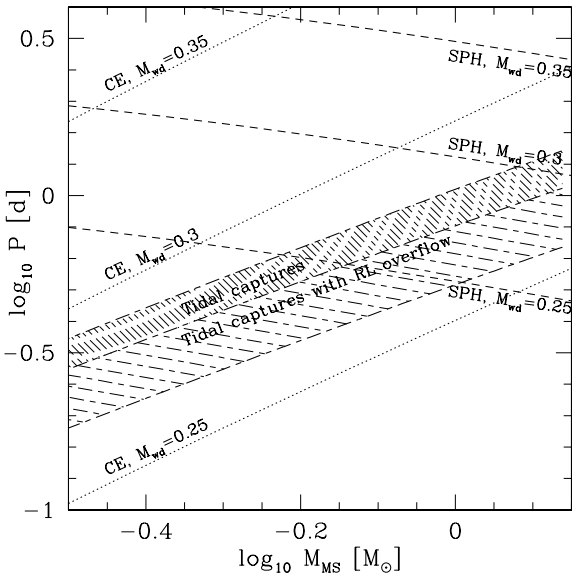


**Figure 5.** Formation of WD–MS binaries via physical collisions and TCs. The hatched area shows binaries formed via TC with a 0.6-$M_\odot$ WD. In the dense hatched area, the MS star did not overflow its Roche lobe at the minimum approach during the TC. The dashed lines show binaries formed via physical collisions of an MS star and a 0.8-$M_\odot$ RG, for different core masses, using parametrized results of SPH simulations (for illustrative purposes, we show only the case of the impact parameter to be 0.54 of the RG radius with corresponding post-collisional eccentricity of 0.7). The dotted lines show binaries formed via physical collisions of an MS star and a 0.8-$M_\odot$ RG, for different core masses, assuming CE approach ($\alpha_{\rm CE} = \lambda = 1$).

1/3. We note that the parameter space for tidally captured binaries where the MS star does not overfill its Roche lobe at the closest approach is very small (see Fig. 3). We note that this is an optimistic estimate, as the captured star can also be destroyed during the chaotic phase of the tidal energy damping (Mardling 1995). Most tidally captured binaries can be brought to contact by MB before either the next encounter occurs, or the MS star evolves away from the MS.

An eccentric binary can be formed via an exchange encounter or a physical collision; eccentricity can also be increased via the cumulative effect of fly-by encounters. For binaries formed through MS–RG collisions, the post-exchange binary separation, $a_{\rm f}$, as well as post-exchange eccentricity, $e_{\rm f}$, depends on the closest approach $p$ (Lombardi et al. 2006) and can be estimated using results of SPH simulations. The simulations were performed for seven models of RGs of two initial masses and at different stages of their evolution, including two subgiant models (cf. previous attempts where only relatively evolved RGs were considered, e.g. Davies, Benz & Hills 1991; Rasio & Shapiro 1991); the resolution of the models is up to $6 \times 10^4$ particles. The results are presented in the convenient form that allowed the parametrization. These simulations were done for physical collisions of an NS and an RG, and therefore are not straightforwardly applicable for the physical collisions of an MS star and an RG. We therefore study how strongly the choice of the treatment can affect the final results. We consider the following two prescriptions.

(i) Using a CE prescription:

$$\frac{(M_{\rm rg}+M_{\rm ms})v_\infty^2}{2} + \alpha_{\rm CE}\frac{GM_{\rm wd}M_{\rm ms}}{2a_{\rm f}} = \frac{GM_{\rm rg}(M_{\rm rg}-M_{\rm wd})}{\lambda R_{\rm rg}}. \qquad (4)$$

© 2006 The Authors. Journal compilation © 2006 RAS, MNRAS

Here, $M_{\rm rg}$, $M_{\rm ms}$ and $M_{\rm wd}$ are the masses of the RG, MS star and RG core that will become a WD, respectively, in $M_\odot$; $R_{\rm RG}$ is the RG radius; $\alpha_{\rm CE}$ is the CE efficiency parameter; and $\lambda$ is the CE parameter that connects a star's binding energy with its parametrized form. We assume that after a CE event the binary is not eccentric.

(ii) Using parametrized results from SPH simulations:

$$e_{\rm f} = 0.88 - \frac{p}{3R_{\rm RG}}, \tag{5}$$

$$a_{\rm f} = \frac{p}{3.3\left(1-e_{\rm f}^2\right)}. \tag{6}$$

As the parametrized SPH simulations were done for a limited set of mass ratios, we also check the energy balance. When we consider the case of the second treatment, we choose the minimum binary separation from equations (4) and (6), as at small masses the extrapolated prescription from SPH simulations can lead to the formation of binaries with artificial energy creation. Also, in the case when an MS star at the pericentre overfills its Roche lobe, we destroy the MS star instead of forming a binary. This is consistent with the results of SPH simulations for physical collisions of an RG and an MS star (J. Lombardi 2005, private communication).

In Fig. 5, we also show possible binary periods for binaries formed via physical collisions with an RG. Note that it is hard to form a relatively close MS–WD binary (one that is able to start MT within a few Gyr) with a WD more massive than 0.3 $M_\odot$ via either prescription. Also, in binaries with the mass ratio $\gtrsim$3, Roche lobe overflow leads to delayed dynamical instability and a binary merger. This limits the MS star mass to $\lesssim 0.9$ $M_\odot$. Therefore, the CV progenitors from the channel of physical collisions of RGs and MS stars are expected to initially have rather low-mass WD accretors, and donor star masses $\lesssim 0.9$ $M_\odot$. Therefore, metallicity variations should not affect this channel strongly. The evolutionary stage during He core burning lasts almost the same time as the RG branch; however, He core stars of $\lesssim 2$ $M_\odot$ are a few times more compact than those at the end of the RG branch and have a larger core than that during RG evolution. Therefore, a collision between an He core burning star and an MS star also favours the formation of a WD–MS binary that is close enough to become a CV. This channel mainly provides binaries with a WD mass at the start of accretion of about 0.5 $M_\odot$ (just a bit above the core mass at the time of He core flash).

On the other hand, there are not many single WDs of such small masses present in a GC core. A WD with mass $\lesssim 0.3$ $M_\odot$ cannot (yet) be formed in single star evolution – it must evolve via either a CE event or a physical collision. A binary containing such a WD is very hard and has $\tau_{\rm coll} \geqslant 10$ Gyr. If an encounter occurs, it is more likely to result in a merger rather than an exchange. We therefore expect that most CVs with a low-mass WD companion will be formed either through a CE event (in a primordial binary or in a dynamically formed binary with $P \sim$ 10–100 d), or as a result of a physical collision, but not via direct exchange encounter.

A typical binary formed via an exchange encounter has $e \approx 0.7$. In order to become a CV within 2 Gyr (or before the next encounter), it should have a post-encounter period of a few days (see also Fig. 4). According to energy conservation during an exchange encounter (Heggie, Hut & McMillan 1996), and assuming that during an exchange encounter the less-massive companion is replaced by the more-massive intruding star, the post-encounter binary separation will be larger than that of pre-encounter. The domain of pre-encounter binaries that will be able to form a CV–progenitor binary via only exchange encounter is therefore limited to very short period binaries (with correspondingly long collision times), and these binaries are very likely to experience a physical collision rather than an exchange (Fregeau et al. 2004).

Let us consider the possibilities for an initially wider dynamically formed binary than that shown in Fig. 4 to evolve towards MT. For definiteness, we consider a binary consisting of a 1-$M_\odot$ MS star and a 0.6-$M_\odot$ WD with an initial period of 10 d. There are two kinds of post-formation dynamical effects that can happen during fly-by encounters: (i) binary hardening; and (ii) eccentricity pumping. Even if each hardening encounter could reduce the orbital separation by as much as 50 per cent, the hardening of this binary from 10 to 1 d (at this period MB starts to be efficient) will take about 20 Gyr. In the case of eccentricity pumping (assuming no binary energy change), the mean time between successive collisions stays at $\tau_{\rm coll} \leqslant 1$ Gyr and, therefore, a binary can experience many encounters. If the acquired eccentricity $e \geqslant 0.95$, the binary can shrink through GW emission even if its initial period is larger than 10 d. The last possibility for such a wide dynamically formed binary to become a CV is a CE event that happens in a post-exchange MS–MS binary.

### 2.3 Dynamical formation of AM CVn systems

For the evolution of WD–WD binaries, we adopt that only GWs are important as a mechanism of angular momentum loss and neglect the possibility of tidal heating. The maximum possible periods for different post-encounter eccentricities are shown on Fig. 6.

Let us first examine a WD–WD binary formation via direct exchange. Again, as in the case of MS–WD binaries, a typical eccentricity is $e \sim 0.7$ and the separation is comparable to the pre-exchange separation. The collision time for both pre-encounter and post-exchange binaries is so long that both binary hardening and exchanges are very rare events. The main difference with MS–WD binaries is that post-exchange WD–WD binary periods that will allow a binary to evolve to MT are several times smaller for the same

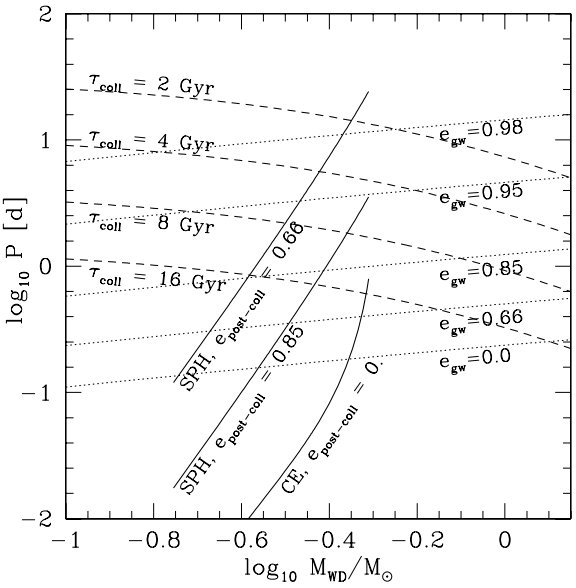


**Figure 6.** The fate of post-encounter WD–WD binaries where the primary is a WD of 0.6 $M_\odot$. $P$ is the post-encounter orbital period and $M_{\rm WD}$ is the mass of the WD secondary. The dashed lines show the binary periods for constant collision times and the dotted lines delineate the binaries that will begin MT within 2 Gyr due to GW emission for different post-encounter eccentricities. The solid lines show binaries of different eccentricities that can be formed through a collision between a WD of 0.6 $M_\odot$ and an RG of 0.8 $M_\odot$ ($\alpha_{\rm CE}\,\lambda = 1$).

© 2006 The Authors. Journal compilation © 2006 RAS, MNRAS

eccentricities. Therefore, the exchange channel producing a post-exchange binary consisting of two WDs seems to be very unlikely.

A more important channel seems to be the case of an exchange encounter that leads to the formation of an MS–WD binary. If the MS star is massive enough to become an RG during the cluster lifetime, such a binary can evolve through CE and form a close WD–WD binary.

The second important channel is again a physical collision, involving a single WD with an RG (see Fig. 6, where we show possible outcomes of such a collision). We note that both treatments (parametrized SPH results and CE prescription) lead to the formation of WD–WD binaries that are roughly equally likely to start the MT.

We therefore expect that only a post-CE system can become an AM CVn, where the post-CE system could be from a primordial binary, a post-collision binary, or a dynamically formed binary.

## 3 METHODS AND ASSUMPTIONS

For our numerical simulations of GCs, we use a Monte Carlo approach described in detail in Ivanova et al. (2005a). The method couples the binary population synthesis code STARTRACK (Belczynski et al. 2002, 2005c), a simple model for the cluster, and a small $N$-body integrator for accurate treatment of all relevant dynamical interaction processes (FEWBODY, Fregeau et al. 2004). The main update of the code is the treatment of physical collisions with an RG, for which we now use the parametrized results of SPH simulations from Lombardi et al. (2006) as described in Section 2.2. In our code, we keep a complete record of all events that happen to any cluster star, dynamical (like collisions, TCs and exchanges, as well as changes of the binary eccentricity or the binary separation after a fly-by encounter), or evolutionary (like CE events, MTs, or SN explosions). This helps to analyse the final populations and understand what factors played the most significant role in their formation.

The 'standard' cluster model in our simulations has initially $N = 10^6$ stars and initial binary fraction of 100 per cent. The distribution of initial binary periods is constant in the logarithm between contact and $10^7$ d and the eccentricities are distributed thermally. We want to stress here that about two-thirds of these binaries are soft initially (the binary fraction provided by only hard binaries gives an initial binary fraction of about 20 per cent if the one-dimensional velocity dispersion is 10 km s$^{-1}$) and most very tight binaries are destroyed through evolutionary mergers. Our initial binary fraction is therefore comparable to the initial binary fractions that are usually used in $N$-body codes, where it is assumed for simplicity that very soft binaries will not live long as binaries and will only slow down the simulations. For more detailed discussion on the choice of the primordial binary fraction, see Ivanova et al. (2005a).

For single stars and primaries, we adopted the broken power-law initial mass function (IMF) of Kroupa (2002) and a flat mass-ratio distribution for secondaries. The initial core mass is 5 per cent of the cluster mass and, assuming initial mass segregation, an average object in the core is about twice as massive as an average cluster star. At the age of 11 Gyr the mass of such a cluster in our simulations is $\sim 2 \times 10^5$ M$_\odot$ and is comparable to the mass of typical GCs in our Galaxy.

We adopt a core number density $n_c = 10^5$ pc$^{-3}$ (this corresponds to $\rho_c \approx 10^{4.7}$ M$_\odot$ pc$^{-3}$ at the ages of 7–14 Gyr), a half-mass relaxation time $t_{rh} = 1$ Gyr and a metallicity $Z = 0.001$. The characteristic velocities are taken as for a King model $W_0 = 7$ for the cluster of this mass. We take a one-dimensional velocity dispersion $\sigma_1 = 10$ km s$^{-1}$ and an escape velocity from the cluster $v_{esc} = 40$ km s$^{-1}$. If, after an interaction or SN explosion, an object in the core acquires a velocity higher than the recoil velocity $v_{rec} = 30$ km s$^{-1}$, an object is moved from the core to the halo. The ejection velocity for objects in the halo is $v_{ej,h} = 28$ km s$^{-1}$. This 'standard' model represents a typical dense GC in our Galaxy.

In addition to the 'standard' model, we also considered cluster models with the following modifications.

(i) A metal-rich cluster with $Z = 0.02$ ('metal-rich');
(ii) central density $n_c = 10^4$ pc$^{-3}$ ('med-dens') or $n_c = 10^3$ pc$^{-3}$ ('low-dens');
(iii) initial binary fraction 50 per cent ('BF05');
(iv) RVJ MB ('fast MB');
(v) treatment of physical collision using a CE prescription (' CE coll'); and
(vi) 47 Tuc type cluster, characterized by a higher density $\rho_c = 10^{5.2}$ M$_\odot$ pc$^{-3}$, higher metallicity $Z = 0.0035$, $\sigma_1 = 11.5$ km s$^{-1}$, $v_{esc} = 57$ (with the recoil velocity of 52 km s$^{-1}$ and $v_{ej,h} = 24$ km s$^{-1}$) and $t_{rh} = 3$ Gyr ('47 Tuc').

'47 Tuc' model describes the GC where currently the largest CV population is identified. In order to find a better match with the observations, we examined several variations of this model. In particular, we considered a model with an initial binary population of 50 per cent ('47 Tuc+BF05'), and a model with an initial binary population of 50 per cent, and the initial core has a smaller mass – 2 per cent, reflecting the effect of a longer half-mass relaxation time on the initial population ('47 Tuc+SCBF05'). We also examined the sensitivity of the final CV production to the CE efficiency parameter, considering the case with $\alpha_{CE}\lambda = 0.1$('47 Tuc+$\alpha_{CE}$ $\lambda$'). For the complete list of models, see Table 1. As the dynamical properties of all our models remain frozen in time, they may lack some effects of cluster dynamical evolution. We discuss these effects in Section 4.1.3.

In order to estimate the effects of dynamics on the population, we also ran the same population as in our 'standard' model ($Z = 0.001$), but without dynamics ('non-dyn'). In order to compare to a field population, we considered the population of stars with solar metallicity $Z = 0.02$ and with different times of star formation, assuming flat star formation rate through last 10 Gyr ('field'). In 'non-dyn' model, all stars are formed at the zero age, like in GCs.

## 4 NUMERICAL RESULTS

### 4.1 Formation channels of CVs

#### *4.1.1 Main formation channels in the 'standard' model*

In Fig. 7, we show the formation channels for all CVs that are present in a typical cluster (our 'standard' model) at the age of 10 Gyr. Most of these CVs are too dim to be detected, and we consider separately the population of CVs that can be detectable according to present observational limits, considered specifically for the GC 47 Tuc. For the limiting X-ray luminosity, we take $L_X \gtrsim 3 \times 10^{30}$ erg s$^{-1}$ (Grindlay et al. 2001a), and the limiting bolometric luminosity of the donor $L_d \gtrsim 0.06$ L$_\odot$, set by the limiting magnitude of *HST* in the cluster core (Edmonds et al. 2003a).

We label channels in the following way. The first character indicates the last major dynamical event affecting the binary before it becomes a CV in the core, as follows: (1) entering the core (primordial binary); (2) companion exchange during a binary encounter; (3) merger during a binary encounter; (4) physical collision with an RG during a binary encounter that resulted in a tight binary formation

© 2006 The Authors. Journal compilation © 2006 RAS, MNRAS

**Table 1.** Models.

| | $n_c$ | $t_{rh}$ | $Z$ | $\sigma_1$ | $f_b^0$ (per cent) | $m_{core}^0$ (per cent) | Coll | $\alpha_{CE}\,\lambda$ | MB |
|---|---|---|---|---|---|---|---|---|---|
| Standard | $10^5$ | 1.0 | 0.001 | 10 | 100 | 5 | SPH | 1.0 | IT03 |
| Metal-rich | · | · | 0.02 | · | · | · | · | · | · |
| Med-dens | $10^4$ | · | · | · | · | · | · | · | · |
| Low-dens | $10^3$ | · | · | · | · | · | · | · | · |
| Fast MB | · | · | · | · | · | · | · | · | RVJ |
| CE coll | · | · | · | · | · | · | CE | · | · |
| BF05 | · | · | · | · | 50 | · | · | · | · |
| 47 Tuc | $2\times10^5$ | 3.0 | 0.0035 | 11.5 | · | · | · | · | · |
| 47 Tuc+BF05 | $2\times10^5$ | 3.0 | 0.0035 | 11.5 | 50 | · | · | · | · |
| 47 Tuc+SCBF05 | $2\times10^5$ | 3.0 | 0.0035 | 11.5 | 50 | 2 | · | · | · |
| 47 Tuc+$\alpha_{CE}\,\lambda$ | $2\times10^5$ | 3.0 | 0.0035 | 11.5 | · | · | · | 0.1 | · |

Notations: $n_c$ – core number density (per pc $^3$), $t_{rh}$ – half-mass relaxation time (Gyr), $Z$ – metallicity, $\sigma_1$ – one-dimensional velocity dispersion (km s$^{-1}$), $f_b^0$ – initial binary fraction, $m_{core}^0$ – initial core mass in units of the total cluster mass, Coll - how the collisions are treated (using SPH or CE prescription, see the text), $\alpha_{CE}\,\lambda$ – CE efficiency, MB – adopted prescription for MB (see the text). The symbol · means that the value is the same as in the standard model.

with an RG core as a companion; (5) TC; and (6) physical collision of a single MS star with a single RG. The second character indicates a sub-channel by which the binary was modified after the last major dynamical event occurred: (1) stands for all subchannels where no strong evolutionary or dynamical event occurred; (2) eccentricity of the formed binary was increased via binary–binary encounters; (3) CE occurred; and (4) a previous MT episode played the most important role in the orbital decay.

The *primordial channel* (**channel 1**) – provides 37 per cent of all CVs that are present in the cluster core (42 per cent of detectable CVs). We call this channel primordial as the binary keeps both its initial companions, and no mergers ever occurred to either of them. Only three-fourths of CVs formed via this channel are 'purely' primordial in the sense that they did not experience a significant dynamical encounter throughout their life (**1a**, see also Fig. 7); most of these 'purely' primordial CVs evolved via CE before they entered the core. As was predicted in Section 2.1, very few CVs come from the channel where CE occurred after a binary entered the core (**1c**). One-fifth of all primordial CVs would not evolve via CE or start an MT, unless their eccentricity was increased via fly-by encounters (**1b**). A small fraction of primordial CVs evolved without a CE but with only an MT episode on to an MS star (**1d**), as was described in Section 2.1.

The binary encounters (**channels 2, 3 and 4**) are responsible for the formation of 46 per cent of all CVs, and the same fraction of detectable CVs. In most cases, the binary that participated in the binary encounter was not a primordial binary, but a dynamically formed binary. In more than half of cases, a future accretor had been a companion in at least three different binaries before it acquired its final donor.

The most effective path is the *binary exchange channel* (**channel 2**) – it provides 32 per cent of all CVs. Within this channel, $\sim$40 per cent of post-exchange binaries evolved towards the MT without further significant dynamical or evolutionary events (**2a**), in 20 per cent of them CE occured (**2c**) and in 40 per cent of them the MT started as a result of the eccentricity pumping during subsequent fly-by encounters (**2b**). This is the most efficient channel for eccentricity pumping.

Exchange encounters that lead to CV formation typically occur between the following participants. (i) A single, relatively heavy WD (about 0.7–1.4 $M_\odot$) and an MS–MS binary of total mass $\lesssim 1\,M_\odot$; and (ii) a single, relatively massive MS star (about turn-off mass) and an MS–WD or a WD–WD binary. In the latter case, CE often follows the exchange encounter. The number of successful encounters between an MS star and a WD–WD binary is relatively small, and no successful four-body encounter occurred. Nearly all binaries that proceed via subchannels **2a** or **2b** are WD–MS binaries, and all binaries in subchannel **2c** are MS–MS binaries after the last strong binary encounter. A post-exchange binary typically has a heavier WD than a primordial (post-CE) binary.

A further 13 per cent of CVs are formed in binaries that experienced a physical collision during the last three- or four-body encounter – *binary collisional channel* (**channel 3**), whereas in 1 per cent of cases a physical collision with an RG occurred during the encounter and a binary with the stripped RG core was formed (**channel 4**). In the evolution of post-collisional binaries, the eccentricity change plays a smaller role compared to post-exchange binaries; MT is started due to the evolutionary angular momentum losses.

The *TC channel* (**channel 5**) contributed very little in our standard model. When we looked at all CVs that were formed via TC over all GC ages, we find that a typical WD that captured an MS star is $\sim 1.0 \pm 0.2\,M_\odot$. In our simulation, we allowed a star to overfill its Roche lobe radius by up to one-third during the TC encounter and survive. If all encounters where an MS star overfills its Roche lobe lead to the stars' merger, then the contribution of TCs would be even smaller.

Finally, the *channel of physical collision with RGs* (**channel 6**) provides 15 per cent of all CVs but much smaller fraction of detectable CVs. Eccentricity pumping played a very small role in both TC and physical collision channels. Typical participants of a successful physical collision (leading to CV formation) are an MS star of 0.3–0.9 $M_\odot$ and an RG of about 1–1.7 $M_\odot$ with a core around 0.3 $M_\odot$ or an He core burning giant with a core mass around 0.5 $M_\odot$. CVs formed by this channel are similar to post-CE CVs from primordial binaries. We also compared the results of CV productions in our large model with $10^6$ stars and in the model with three times less stars. We noted that, with the increase in the resolution, the total number and the number of detectable CVs per unit of the core mass slowly decrease. Branching ratios between subchannels within a channel can vary slightly, but the overall picture is the same.

The following are our main findings.

(i) Only $\sim$25 per cent of CVs were formed in binaries that would become CVs in the field.

© 2006 The Authors. Journal compilation © 2006 RAS, MNRAS

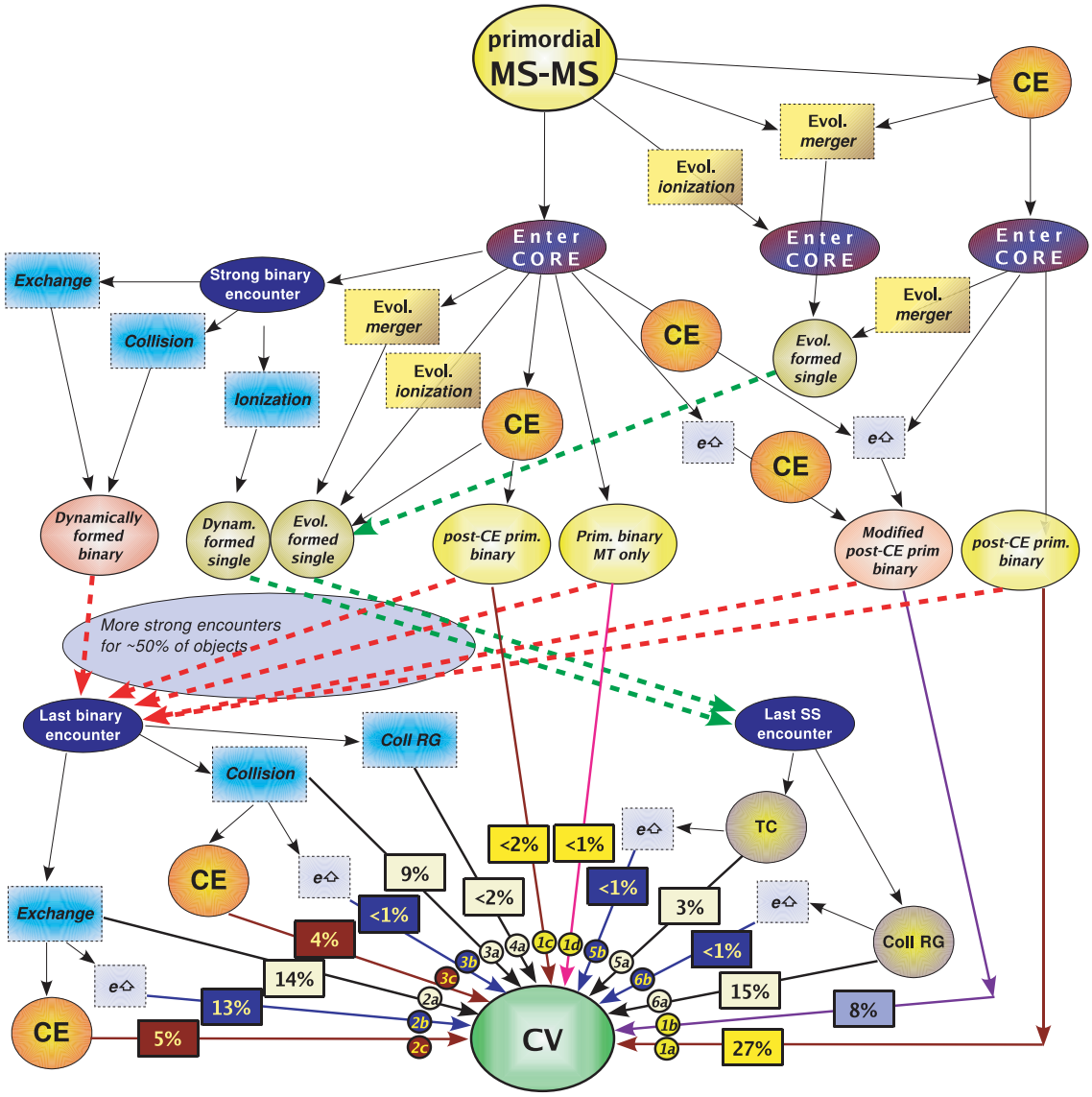


**Figure 7.** Main formation channels of all CVs that are present in a 'standard' cluster at the age of 10 Gyr. Notations: numbers in squares represent contributions from different channels, small circles contain the labels for each channel. 'CE' – common envelope, 'Evol. merger' – evolutionary merger, 'Evol. ionization' – destruction of the binary via an SN explosion, 'e⇑' – increase of the eccentricity during fly-by encounters, 'Strong binary encounter' – three- or four-body encounter with an outcome as exchange, binary destruction ('ionization') or physical collision ('Collision'), 'TC' – tidal capture, and 'Coll RG' – physical collision with an RG.

(ii) In ∼20 per cent of CVs, the main reason for a binary to become a CV was fly-by encounters. These CVs cannot be predicted in simulations where only strong encounters are taken into account.

(iii) In ∼15 per cent of CVs, the WD was formed during dynamical removal of the RG envelope. As this removal is not 'clean', and about 0.1 $M_{\odot}$ (see Lombardi et al. 2006) can remain bound to the RG stripped core, the characteristics of the WD can differ from those formed via a CE.

(iv) 60 per cent of CVs did not evolve via CE, which is the most common formation channel for field CVs.

(v) TCs did not play a significant role.

### *4.1.2 Formation channels in different clusters*

In Table 2, we give details on the formation channels for different cluster models at the same age of 10 Gyr. We note that these numbers fluctuate with time and are not defined precisely (see more below in Section 4.1.3); however, some trends can be identified. We also show the numbers of CVs that are formed in a metal-poor environment ('non-dyn') and in the field. The definition of 'detectable' CVs is not very consistent here, as observational limits for field CVs are not the same as for GCs (and much more poorly defined), but we use the same limits for comparison. It can be seen that dynamics in the 'standard' model leads to an increase in the total CV production by less than a factor of two. On the other hand, the comparison of the 'non-dyn' and 'standard' models is helpful for understanding the formation of halo CVs. All detectable CVs in the 'non-dyn' are heavy, and, due to mass segregation, contribute only to the core CV population. All CVs that are present in the halo are therefore either below the (optical) detection limit, or are detectable CVs that were ejected from the core to the halo after a dynamical encounter.

© 2006 The Authors. Journal compilation © 2006 RAS, MNRAS

**Table 2.** Formation channels of CVs that are present in the cluster cores of different models at the age of 10 Gyr.

| Channel | 1a | 1b | 1c | 2a | 2b | 2c | 3a | 3b | 3c | 4a | 5a | 6a | Total | Detec |
|---|---|---|---|---|---|---|---|---|---|---|---|---|---|---|
| Standard | 0.271 | 0.077 | 0.013 | 0.135 | 0.129 | 0.052 | 0.090 | 0.006 | 0.039 | 0.013 | 0.026 | 0.148 | 209 | 47 |
| Metal-rich | 0.204 | 0.056 | 0.031 | 0.148 | 0.143 | 0.046 | 0.051 | 0.015 | 0.015 | 0.020 | 0.031 | 0.230 | 265 | 16 |
| Med-dens | 0.327 | 0.253 | 0.167 | 0.111 | 0.012 | 0.056 | 0.031 | 0.019 | 0.006 | 0.006 | 0.000 | 0.006 | 193 | 35 |
| Low-dens | 0.404 | 0.066 | 0.456 | 0.037 | 0.000 | 0.007 | 0.015 | 0.000 | 0.015 | 0.000 | 0.000 | 0.000 | 156 | 26 |
| Fast MB | 0.190 | 0.103 | 0.017 | 0.086 | 0.190 | 0.172 | 0.034 | 0.017 | 0.000 | 0.017 | 0.052 | 0.103 | 79 | 15 |
| CE coll | 0.212 | 0.106 | 0.006 | 0.159 | 0.194 | 0.041 | 0.041 | 0.029 | 0.029 | 0.006 | 0.000 | 0.176 | 230 | 47 |
| BF05 | 0.206 | 0.119 | 0.024 | 0.135 | 0.135 | 0.056 | 0.040 | 0.032 | 0.024 | 0.024 | 0.008 | 0.175 | 162 | 36 |
| 47 Tuc | 0.135 | 0.094 | 0.000 | 0.250 | 0.146 | 0.073 | 0.042 | 0.042 | 0.021 | 0.031 | 0.000 | 0.156 | 275 | 37 |
| 47 Tuc+BF05 | 0.143 | 0.057 | 0.014 | 0.171 | 0.143 | 0.029 | 0.014 | 0.043 | 0.029 | 0.000 | 0.043 | 0.300 | 190 | 35 |
| 47 Tuc+SCBF05 | 0.071 | 0.114 | 0.000 | 0.100 | 0.114 | 0.057 | 0.014 | 0.014 | 0.014 | 0.014 | 0.029 | 0.443 | 237 | 27 |
| 47 Tuc+$\alpha_{\rm CE}$ $\lambda$ | 0.170 | 0.057 | 0.011 | 0.182 | 0.125 | 0.045 | 0.034 | 0.011 | 0.011 | 0.023 | 0.023 | 0.307 | 253 | 40 |
| non-dyn | | | | | | | | | | | | | 124 | 16 |
| field | | | | | | | | | | | | | 117 | 3 |

*Notes.* Notations for channels – see the text in Section 4.1.1 and also Fig. 7. 'Total' is the number of CVs and 'Detec' is the number of detectable CVs, both numbers are scaled per 50 000 $M_\odot$ stellar population mass in the core.

In the case of the 'metal-rich' model, the turn-off mass at 10 Gyr is larger than that in the 'standard' model – there are more-massive stars in the core; the ratio between the total numbers of CVs in the two models is roughly the ratio between their turn-off masses at this age.

As was expected, the role of purely primordial CVs (**channel 1a**) decreases in importance when density increases (see 'standard', 'med-dens' and 'low-dens' models), although their absolute number is about the same for all three models – once a CV is formed outside the core, it is hard to destroy it in the core. On the other hand, the number of systems that experience CE after entering the core (**1c**) increases as the density decreases, since it is easier for pre-CE systems to survive in a less-dense environment. The production of almost all channels via dynamical encounters decreases with density, except for channel 1b, where only non-strong encounters are involved. Overall, the total number of CVs in the core does not depend strongly on the core density, as the dynamical destruction of primordial binaries that would produce CVs, and the dynamical production of CVs, compensate each other.

The 'fast MB' model shows the greatest difference with the 'standard' model in the total number of CVs that are present in the cluster core: the 'standard' model has about three times more CVs, both total and detectable, although the number of CVs that are ever formed in the core is slightly smaller. The 'fast MB' model employs the prescription of MB with faster angular momentum loss than that in the case of the standard model and, therefore, the duration of the CV stage is shorter.

The 'CE coll' model does not show significant differences with our 'standard' model.

The 'BF05' model shows that CV formation is reduced mainly for primordial CVs and for CVs produced via binary encounters. The number of CVs produced via physical collisions between single stars is about the same.

The results for '47 Tuc' are due to a mixture of several conditions: the higher core number density favours dynamical formation, and the higher metallicity gives a wider mass range over which MB operates on the donor star. Variation in initial conditions, such as a smaller binary fraction, does not lead to significant differences except that the relative role of binaries becomes smaller than the role of physical collisions. Some decrease in the number of detectable CVs occurs when we start with a smaller initial core.

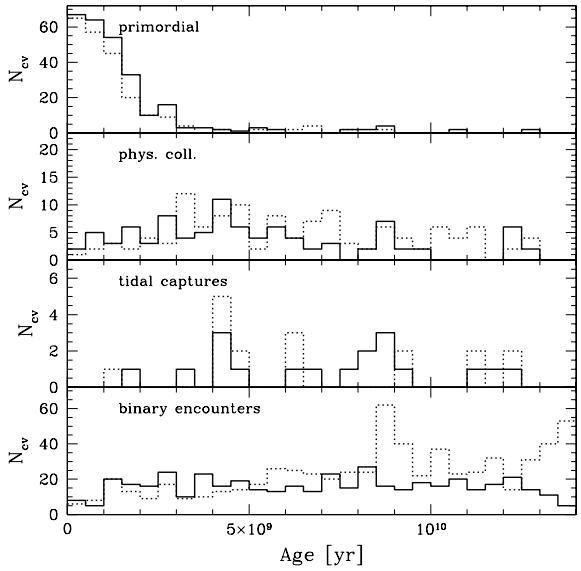


**Figure 8.** Formation of CVs via different channels. The solid line shows the case of 'standard' model; the dotted line shows that of 'metal-rich' model.

### *4.1.3 Formation channels at different cluster ages*

In Fig. 8, we show the formation rate of CVs via different channels throughout the life of a cluster (indicating the time when a dynamical event occurred, or, for primordial binaries, the time when a CE happened). In Fig. 9, we show the rate of appearance of CVs (start of MT) as a function of time.

The primordial channel produces most of its CVs at the beginning of the cluster evolution, though the appearance of primordial CVs is distributed uniformly in time. This contrasts with binary encounter channels, where the formation occurs approximately constant in time, but the rate of CV appearance grows after 7 Gyr. A similar delay in the appearance can be seen for CVs formed via TCs.

In Fig. 10, we show the number of CVs that stop MT for different reasons: (1) end of MT either due to the star's contraction (usually occurs with CVs where a donor is an RG) or due to evolutionary merger of the binary; (2) explosion of the WD as Type Ia supernova (SN Ia) or sub-Chandrasekhar SN explosion, or accretion-induced

© 2006 The Authors. Journal compilation © 2006 RAS, MNRAS

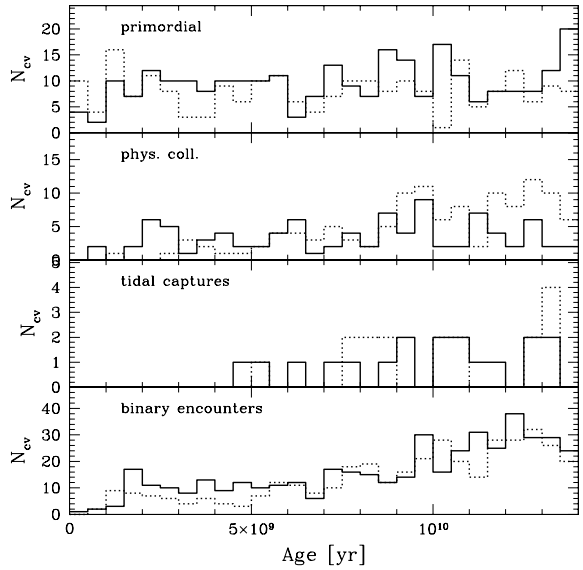


**Figure 9.** Appearance of CVs (time that MT starts) formed via different channels. Notations as in Fig. 8.

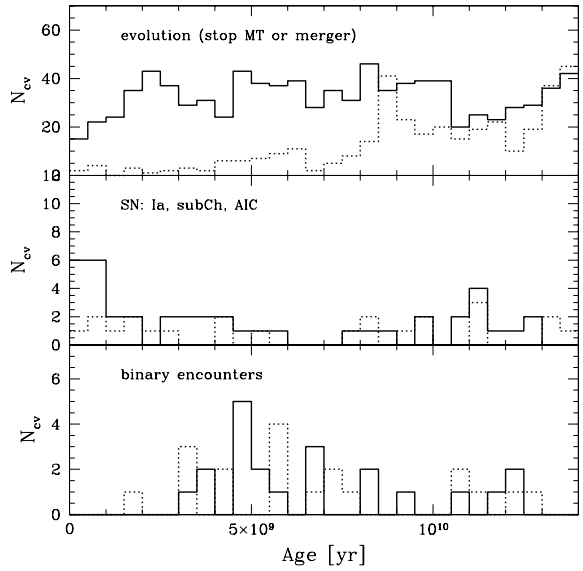


**Figure 10.** Destruction of CVs. Notations as in Fig. 8.

collapse (AIC); (3) end of MT due to a strong dynamical encounter. Most CVs stop MT due to an evolutionary reason, while the number of SN explosions is also relatively high and is comparable to the number of CVs destroyed by dynamical encounters (for more detail on how SNe Ia are calculated, see Section 4.4 and Belczynski, Bulik & Ruiter 2005b).

In Table 3, we show a detailed representation of CV formation by different channels in the 'standard' model at different cluster ages. We note a peak in the number of detectable CVs at the age of 4 Gyr, and that the total number of CVs increases steadily until the age of 8 Gyr and then stays constant. The weight of different channels in the relative numbers of appearing CVs does not change dramatically during the cluster evolution.

Understanding the connection of CV production with the cluster density, age and the time-delay between the pre-CV binary formation and the actual CV appearance helps us to predict how dynamical cluster evolution will affect CV production. For example, in the case of a gradual density increase, the number of CVs that can be detected now would correspond to the cluster conditions several Gyr ago, when the cluster was less dense. So, for two clusters with the same current central density, the one that is undergoing contraction *now* will contain less CVs. It is interesting to note that if the cluster underwent core collapse very recently, less than 1 or 2 Gyr ago, this cannot yet strongly increase the current number of dynamically produced CVs; however, their immediate depletion rate due to encounters (e.g. binary destructions, recoil, ejection) will increase. As a result, the cluster core will appear to have even *less* CVs than it had with a lower density before core collapse.

### 4.2 Population characteristics of CVs

#### *4.2.1 Periods and masses*

In Figs 11 and 12, we show mass and period distributions for 'standard' and '47 Tuc' cluster models, as well as for the population evolved without dynamics. A remnant of the primordial population of CVs in cluster cores follows the distribution of primordial CVs evolved without dynamics at the same age. However, the distribution of dynamically formed CVs shows signs of younger (non-dynamical) CV populations, and also is more populated at the high-mass end. For 47 Tuc, we also show the periods of the identified CVs, which have a distribution consistent with the period distribution of the 'detectable' CVs in our simulations.

#### *4.2.2 MT rates and X-ray luminosities*

We compare the distribution of orbital periods versus 0.5–2.5 keV X-ray luminosity for our simulation of 47 Tuc and observations of CVs in GCs (see Figs 13 and 14).[2] Observationally, a few CVs have measured orbital periods. For real CVs with unknown periods, only the X-ray luminosity is shown. To obtain the X-ray luminosity of simulated CVs for comparison to observations, we use the accretion model from Patterson & Raymond (1985) for 0.5–4 keV and scale the luminosity to 0.5–2.5 keV assuming a flat energy distribution within the band:

$$L_{\rm X}(0.5-2.5\ {\rm keV}) = 0.066\frac{GM_{\rm wd}.5\dot{M}}{2R_{\rm wd}}, \qquad (7)$$

where $\dot{M}$ is the MT rate and $R_{\rm wd}$ is the radius of the WD. The simulations show reasonable agreement with the observations.

However, this picture so far does not explain the rare occurrence of DNOs in GC CVs, in comparison to the field. Therefore, other properties of these systems must be explored to identify the distinguishing characteristics.

In Fig. 15, we show MT rates in CVs in 'standard' model, in the '47 Tuc' model and for the field. Although MT rates in our GC simulations do not exceed $10^{-9}$ $M_\odot$ yr$^{-1}$, and field CVs can have higher MT rates, this result may be due to small number statistics. We therefore do not find significant differences between MT rates in GC CVs and field CVs. For our GC CVs, all MT rates are such that the accretion disc is partially ionized and unstable, in accordance with the disc instability model. We adopt the viscosity parameters $\alpha_{\rm hot} = 0.1$ and $\alpha_{\rm cold} = 0.01$, for hot and stable disc states, respectively. Therefore, all our CVs should produce DNOs.

[2] Note that our '47 Tuc' represents a cluster similar to 47 Tuc but five times less massive.

© 2006 The Authors. Journal compilation © 2006 RAS, MNRAS

**Table 3.** Formation channels of CVs that are present in the 'standard' cluster core at different ages.

| Channel | 1a | 1b | 1c | 2a | 2b | 2c | 3a | 3b | 3c | 4a | 5a | 6a | Total | Detec |
|---|---|---|---|---|---|---|---|---|---|---|---|---|---|---|
| 1 Gyr | 0.250 | 0.000 | 0.000 | 0.000 | 0.250 | 0.250 | 0.000 | 0.000 | 0.000 | 0.000 | 0.000 | 0.250 | 15 | 7 |
| 2 Gyr | 0.111 | 0.074 | 0.037 | 0.259 | 0.111 | 0.185 | 0.000 | 0.000 | 0.037 | 0.000 | 0.000 | 0.185 | 84 | 37 |
| 3 Gyr | 0.185 | 0.046 | 0.015 | 0.154 | 0.169 | 0.123 | 0.015 | 0.000 | 0.015 | 0.031 | 0.015 | 0.231 | 170 | 62 |
| 4 Gyr | 0.200 | 0.078 | 0.022 | 0.167 | 0.133 | 0.133 | 0.022 | 0.000 | 0.011 | 0.022 | 0.011 | 0.200 | 203 | 76 |
| 5 Gyr | 0.190 | 0.076 | 0.029 | 0.162 | 0.086 | 0.095 | 0.057 | 0.010 | 0.019 | 0.019 | 0.019 | 0.229 | 210 | 62 |
| 6 Gyr | 0.214 | 0.077 | 0.026 | 0.162 | 0.103 | 0.060 | 0.051 | 0.009 | 0.026 | 0.026 | 0.017 | 0.231 | 211 | 56 |
| 7 Gyr | 0.268 | 0.049 | 0.016 | 0.163 | 0.114 | 0.041 | 0.049 | 0.008 | 0.024 | 0.024 | 0.016 | 0.220 | 204 | 43 |
| 8 Gyr | 0.284 | 0.061 | 0.014 | 0.128 | 0.122 | 0.068 | 0.054 | 0.007 | 0.041 | 0.020 | 0.014 | 0.182 | 228 | 44 |
| 9 Gyr | 0.268 | 0.067 | 0.013 | 0.128 | 0.134 | 0.060 | 0.074 | 0.007 | 0.047 | 0.020 | 0.013 | 0.161 | 214 | 40 |
| 10 Gyr | 0.271 | 0.077 | 0.013 | 0.135 | 0.129 | 0.052 | 0.090 | 0.006 | 0.039 | 0.013 | 0.026 | 0.148 | 209 | 47 |
| 11 Gyr | 0.253 | 0.084 | 0.006 | 0.157 | 0.139 | 0.054 | 0.078 | 0.006 | 0.042 | 0.012 | 0.030 | 0.139 | 212 | 51 |
| 12 Gyr | 0.209 | 0.088 | 0.005 | 0.165 | 0.181 | 0.049 | 0.066 | 0.016 | 0.033 | 0.005 | 0.027 | 0.154 | 221 | 41 |
| 13 Gyr | 0.203 | 0.091 | 0.005 | 0.188 | 0.162 | 0.056 | 0.066 | 0.030 | 0.030 | 0.010 | 0.025 | 0.132 | 228 | 34 |
| 14 Gyr | 0.199 | 0.131 | 0.000 | 0.184 | 0.155 | 0.039 | 0.068 | 0.044 | 0.029 | 0.010 | 0.019 | 0.121 | 229 | 43 |

*Note*. Notations are as in Table 2.

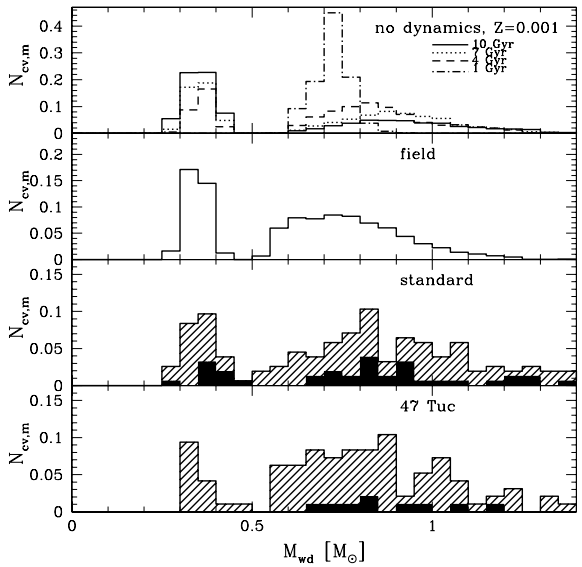


**Figure 11.** The mass-distribution of hydrogen-accreting WDs. The hatched area corresponds to dynamically formed binaries; the solid filled area corresponds to systems formed directly from primordial binaries. The top panel shows the case with no dynamics (different ages), the second panel from the top shows the compiled field case, the third panel shows the core of the cluster in the 'standard' model and the bottom panel shows the cluster core in the model '47 Tuc'.

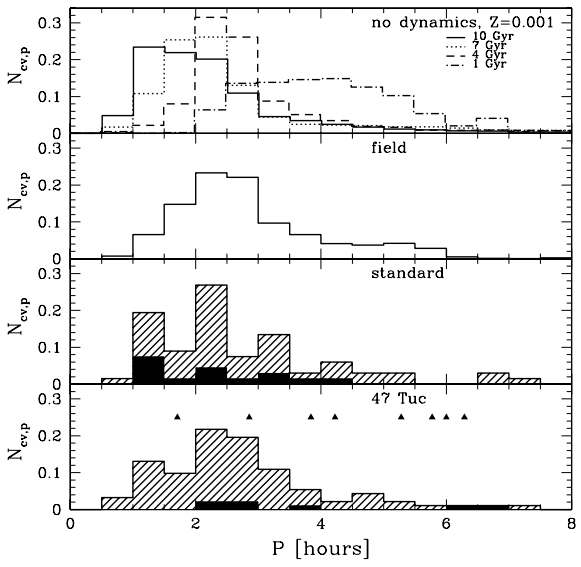


**Figure 12.** The period-distribution of hydrogen-accreting WDs. The hatched area corresponds to dynamically formed binaries; the solid filled area corresponds to systems formed directly from primordial binaries. The top panel shows the case with no dynamics (different ages), the second panel from the top shows the compiled field case, the third panel shows the core of the cluster in the 'standard' model and the bottom panel shows the cluster core in the model '47 Tuc'. The solid triangles indicate the periods of CVs that are identified in 47 Tuc from observations.

Dobrotka et al. (2006) proposed that a combination of low MT rates and moderately strong magnetic fields can explain the absence of DNOs in GCs. Lower MT rates would lead to a rarer occurrence of DNOs, and strong magnetic fields would lead to truncation of the inner disc keeping the disc in the cold stable state. As we do not find systematically lower MT rates for our GC CVs (in fact our MT rates are two orders of magnitude higher than that found in Dobrotka et al. 2006), we estimated the minimum magnetic field required to suppress DNOs (see Fig. 16), using the criterion from Dobrotka et al. (2006):

$$B_{\rm supp} \gtrsim 5.7\times10^{5}{\rm G}\left(\frac{\dot{M}}{10^{-10}\,{\rm M}_{\odot}\,{\rm yr}^{-1}}\right)^{1.16}\left(\frac{M_{\rm wd}}{{\rm M}_{\odot}}\right)^{0.83} \times\left(\frac{0.01\,{\rm R}_{\odot}}{R_{\rm wd}}\right)^{3}. \quad (8)$$

We find that $B_{\rm supp}$ is a slowly increasing function of the WD mass and, for most of the WDs with masses below 1 $M_{\odot}$, is even below $10^6$ G. WDs with $B \lesssim 10^6$ G are not regarded as highly magnetic. It can also be seen that a $10^7$ G field is enough to prevent DNOs in all CVs with the WDs less massive than 1.1 $M_{\odot}$ and the field of $10^8$ G is strong enough to stop DNOs for WDs of all masses.

### 4.3 Formation channels of AM CVn systems

In Table 4, we show the main formation channels for AM CVn systems that occur in different clusters, classifying channels in an analogous manner to Section 4.1.1. The main differences with the formation of CVs are: (i) post-CE channels (including primordial) are more important; (ii) the role of physical collisions for AM CVn

© 2006 The Authors. Journal compilation © 2006 RAS, MNRAS

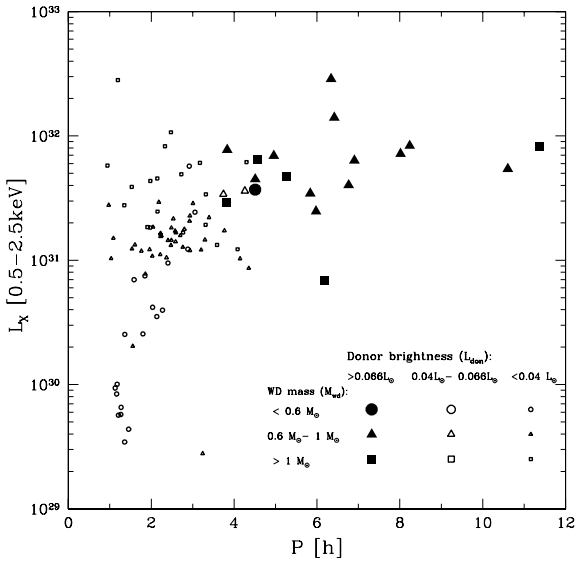


**Figure 13.** Simulated distribution of orbital periods versus 0.5–2.5 keV X-ray luminosity for '47 Tuc' model (at the age of 11 Gyr). The stars are CVs that could be detected, whereas the open circles are CVs that cannot be detected (generally due to the optical faintness of the donor). The shape of the symbol corresponds to the WD mass (squares are for WDs more massive than 1 $M_\odot$, circles are for WDs less massive than 0.6 $M_\odot$, and triangles are for WDs with masses between 0.6 and 1 $M_\odot$).

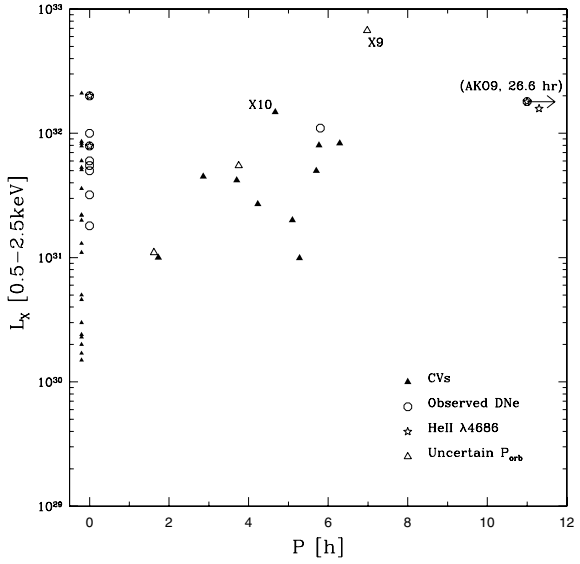


**Figure 14.** Observed distribution of orbital periods versus 0.5–2.5 keV X-ray luminosity for CVs in GCs. Known CVs in GCs, with known X-ray luminosities but without known orbital periods, are plotted at $P = 0$ h or less. CVs that have undergone recorded DNOs are indicated with the circles; CVs with strong He II λ4686 emission (suggesting strong magnetic fields, see the text) are indicated with stars (some are both). Three objects with uncertain periods or CV status (W34 in 47 Tuc might be a millisecond pulsar) are marked as the open triangles; other CVs are indicated with the filled triangles. Data include 23 CVs from 47 Tuc (Edmonds et al. 2003a,b), eight from NGC 6397 (Edmonds et al. 1999; Grindlay et al. 2001b; Kaluzny & Thompson 2003; Shara et al. 2005), seven from NGC 6752 (Pooley et al. 2002; Bailyn et al. 1996), two from M22 (Pietrukowicz et al. 2005), two from M15 (Hannikainen et al. 2005), one from M5 (Hakala et al. 1997; Neill et al. 2002), one from M4 (Bassa et al. 2004), and one from M55 (Kaluzny et al. 2005).

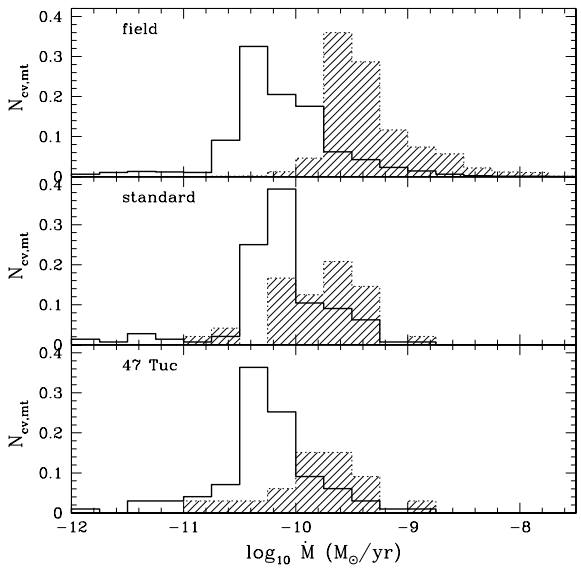


**Figure 15.** MT rates in CVs. The hatched areas indicate detectable CVs. For our no-dynamics model, the detectable CV histogram is increased by a factor of 10, whereas for '47 Tuc' it is increased by a factor of 3. '47 Tuc' is shown at the age of 11 Gyr.

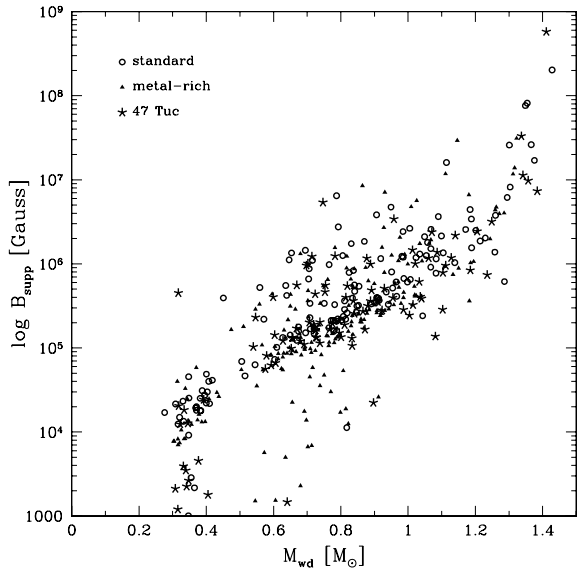


**Figure 16.** The minimum magnetic field $B_{\rm supp}$ required to prevent DNOs for CVs in our simulations. The open circles show CVs in the 'standard' model, the filled triangles show CVs in the 'metal-rich' model, and the stars indicate CVs in the '47 Tuc' model.'47 Tuc' is shown at the age of 11 Gyr; other models are shown at the age of 10 Gyr.

systems is increased; and (iii) binary encounters played a much less significant role.

In most physical collisions, the participants are an RG of 0.9–2.2 $M_\odot$ (the core mass is 0.2–0.3 $M_\odot$) and a WD of $\gtrsim$ 0.6 $M_\odot$. In $\lesssim$20 per cent of physical collisions, the participants are an He core burning giant of 1.7–2.2 $M_\odot$ (the collision in this case leads to the formation of a He star of 0.4–0.55 $M_\odot$) and a heavier WD, generally $\gtrsim$0.9–1.1 $M_\odot$.

Overall, this channel provides AM CVn systems with accretors of masses from 0.8 to 1.4 $M_\odot$ at a cluster age of 10 Gyr. The field

© 2006 The Authors. Journal compilation © 2006 RAS, MNRAS

**Table 4.** Formation channels of AM CVn systems that are present in the 'standard' cluster core at 10 Gyr.

| Channel | 1a | 1b | 1c | 2a | 2b | 2c | 3a | 3b | 3c | 4a | 5a | 6a | Total |
|---|---|---|---|---|---|---|---|---|---|---|---|---|---|
| Standard | 0.385 | 0.068 | 0.000 | 0.051 | 0.090 | 0.030 | 0.013 | 0.013 | 0.064 | 0.064 | 0.009 | 0.265 | 316 |
| Metal-rich | 0.379 | 0.089 | 0.000 | 0.031 | 0.071 | 0.022 | 0.018 | 0.004 | 0.009 | 0.009 | 0.000 | 0.348 | 303 |
| Med-dens | 0.732 | 0.141 | 0.056 | 0.010 | 0.010 | 0.015 | 0.005 | 0.000 | 0.000 | 0.000 | 0.000 | 0.076 | 236 |
| Low-dens | 0.680 | 0.085 | 0.178 | 0.008 | 0.004 | 0.036 | 0.000 | 0.000 | 0.000 | 0.000 | 0.000 | 0.178 | 283 |
| Fast MB | 0.450 | 0.077 | 0.000 | 0.036 | 0.068 | 0.045 | 0.009 | 0.005 | 0.027 | 0.027 | 0.000 | 0.266 | 303 |
| CE coll | 0.474 | 0.123 | 0.000 | 0.035 | 0.082 | 0.023 | 0.006 | 0.012 | 0.018 | 0.018 | 0.012 | 0.211 | 231 |
| BF05 | 0.271 | 0.090 | 0.005 | 0.053 | 0.080 | 0.016 | 0.011 | 0.032 | 0.011 | 0.011 | 0.000 | 0.404 | 242 |
| 47 Tuc | 0.246 | 0.070 | 0.000 | 0.026 | 0.070 | 0.035 | 0.035 | 0.018 | 0.009 | 0.009 | 0.000 | 0.491 | 327 |
| 47 Tuc+BF05 | 0.174 | 0.110 | 0.000 | 0.018 | 0.101 | 0.037 | 0.000 | 0.009 | 0.009 | 0.009 | 0.009 | 0.514 | 296 |
| 47 Tuc+SCBF05 | 0.217 | 0.101 | 0.000 | 0.029 | 0.043 | 0.043 | 0.000 | 0.000 | 0.014 | 0.014 | 0.000 | 0.551 | 233 |
| 47 Tuc+$\alpha_{\rm CE}$ $\lambda$ | 0.252 | 0.078 | 0.000 | 0.000 | 0.117 | 0.029 | 0.019 | 0.010 | 0.058 | 0.058 | 0.000 | 0.427 | 296 |
| Non-dyn | | | | | | | | | | | | | 169 |
| Field | | | | | | | | | | | | | 110 |

*Notes*. Notations for channels are the same as for CVs (see the text in Section 4.1.1 and also Fig. 7). 'Total' is the number of AM CVn systems, the number is scaled per 50 000 $M_\odot$ stellar population mass in the core.

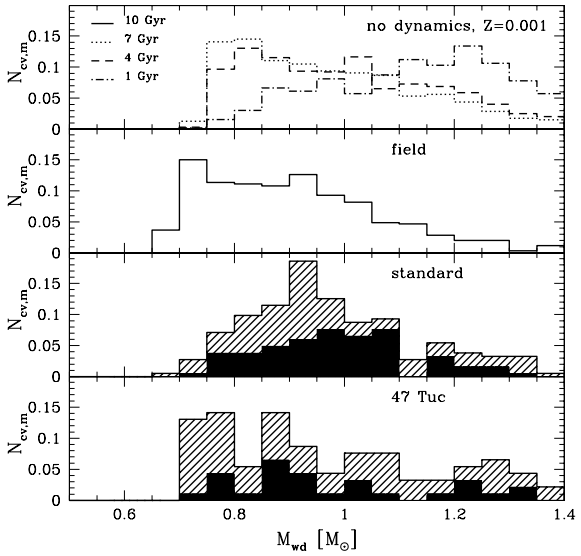


**Figure 17.** The mass-distribution of helium-accreting WDs. The hatched area corresponds to dynamically formed binaries; the solid filled area corresponds to systems formed directly from primordial binaries. The top panel shows the case with no dynamics (different ages), the second panel from the top shows the compiled field case, the third panel shows the core of the cluster in the 'standard' model and the bottom panel shows the cluster core in the model '47 Tuc'.

population of AM CVn systems would have accretors with masses typically between 0.65 and 1.0 $M_\odot$ (Fig. 17, see also Nelemans et al. 2001; Belczynski et al. 2005a). The peak in the accretor mass distribution is shifted from $\sim$0.7 $M_\odot$ in the field population to 0.9 $M_\odot$ in the cluster population.

### 4.4 Explosive events

As the mass distribution of accreting WDs is shifted towards higher masses compared to the field population, it is important to check what effect this has on the rates of: (i) SNe Ia (here, we mean the single-degenerate channel only); (ii) double WD mergers (those for which the total mass $\geqslant M_{\rm Ch} \simeq 1.4$ $M_\odot$); (iii) sub-Chandrasekhar supernovae; and (iv) AIC.

The type of event that occurs depends on the mass and composition of the WD and the rate of MT. If this is a CO WD and experiences stable accretion, it will accumulate mass until it reaches the Chandrasekhar limit and then explodes as an SN Ia. In the case of specific MT rates, the accretion leads to the accumulation of He in the shell (Kato & Hachisu 1999). If sufficient mass is accumulated, it will lead to the ignition of the CO or ONeMg core and disruption of the WD as a sub-Chandrasekhar-mass SN Ia (see Taam 1980; Livne & Glasner 1991; Woosley & Weaver 1994; García-Senz, Bravo & Woosley 1999; Ivanova & Taam 2004). In the case of accretion on to ONeMg WDs, upon reaching the Chandrasekhar limit the WD will undergo AIC and form an NS.

If the donor is another WD and the MT is not stable, the mass of the merger product can exceed the Chandrasekhar limit – these so-called supra-Chandrasekhar mergers could lead either to a Type Ia supernova (double-degenerate channel), or to a merger-induced collapse of the remnant to form an NS and perhaps a millisecond radio pulsar (Chen & Leonard 1993). It was argued as well that in the latter case and, if one of the WDs is magnetic, such mergers will lead to magnetar formation. Such objects may be responsible for the production of the giant flares emitted by soft $\gamma$-repeaters, which can be identified with early-type galaxies. These flares may contribute to a fraction of the observed short-duration burst population at higher redshift (Levan et al. 2006).

If NSs are born with natal kicks, most of them will be ejected from the shallow cluster potential, leaving a few NSs to explain the observed number of millisecond pulsars (Pfahl, Rappaport & Podsiadlowski 2002). In the case of accretion- or merger-induced collapse, the NSs are likely to be formed without a significant kick (Podsiadlowski et al. 2004), and this can relieve the NS 'retention problem'. If double WD mergers do not lead to collapse, they must contribute to the rate of SNe Ia, with potential cosmological implications (for a review see Leibundgut 2001).

The production of supra-Chandrasekhar mergers in our Galaxy was discussed in Hurley, Tout & Pols (2002) and was estimated to be 2.6 per year in the Galactic disc (this is 8.6 per cluster per Gyr in our units). Several free parameters can have strong effects on this result, such as the CE prescription, the IMF, or the adopted star formation history. There are also differences between our models and those of Hurley et al. (2002): (i) their cut-off mass for WD binaries is at the initial mass of 0.8 $M_\odot$; (ii) they choose $\alpha_{\rm CE} = 3$; (iii) they adopted continuous star formation through 15 Gyr (cf ours 10 Gyr); and (iv) our model for accretion on to WDs is more up-to-date (for details, see Belczynski et al. 2005c). Overall, we find that our formation rates for the field are not significantly different

© 2006 The Authors. Journal compilation © 2006 RAS, MNRAS

**Table 5.** Rate of explosive events.

| Event | SN Ia | Supra-Chandrasekhar | Sub-Chandrasekhar | AIC | $NS_{DD}$ | $NS_{AIC}$ |
|---|---|---|---|---|---|---|
| Standard | 2.0 | 9.3 | 7.3 | 3.21 | 118 | 79.2 |
| Metal-rich | 3.48 | 8.2 | 11.7 | 2.73 | 117 | 91.4 |
| Med-dens | 0.48 | 2.4 | 8.0 | 1.45 | 89 | 64.7 |
| Low-dens | 0.00 | 2.9 | 9.8 | 0.72 | 80 | 61.3 |
| Fast MB | 3.48 | 8.2 | 11.7 | 2.73 | 117 | 91.4 |
| CE coll | 0.74 | 7.7 | 8.9 | 2.97 | 117 | 85.1 |
| BF05 | 1.56 | 3.6 | 4.2 | 2.45 | 70 | 45.5 |
| 47 Tuc | 1.22 | 4.9 | 9.3 | 2.44 | 88 | 70.3 |
| 47 Tuc+BF05 | 1.54 | 2.2 | 6.4 | 0.66 | 65 | 42.1 |
| 47 Tuc+SCBF05 | 0.66 | 2.4 | 6.2 | 0.88 | 50 | 36.3 |
| 47 Tuc+$\alpha_{CE}$ $\lambda$ | 2.20 | 3.2 | 8.8 | 1.71 | 87 | 59.6 |
| Non-dyn | 0.00 | 0.7 | 3.2 | 0.00 | 70 | 69.4 |
| Field | 0.50 | 7.7 | 15.1 | 1.58 | 122.17 | 22.8 |

*Notes*. 'SN Ia' is the number of SNe Ia (single-degenerate channel only), 'Supra-Chandrasekhar' is the number of double WD mergers where the total mass is more than 1.4 $M_\odot$, 'Sub-Chandrasekhar' is the number of sub-Chandrasekhar nuclear runaways, 'NS' is the number of NSs that can be potentially formed via double-degenerate ($NS_{DD}$) or AIC ($NS_{AIC}$) channels until the age of 10 Gyr. For cluster models, rates and numbers are given per Gyr per 200 000 $M_\odot$ total cluster mass and are averaged for the ages of 8–12 Gyr. For non-dynamical models, rates and numbers are given for the age of 10 Gyr and for the field model rates and numbers are given after 10 Gyr of continuous star formation.

from those of Hurley et al. (2002) (see Table 5). We also find that our rates are smaller if the star formation is taken not as constant, but with one (or several) star formation bursts that ended several Gyr ago.

The enhanced production rate of double WD mergers in dense stellar clusters was first discussed in detail by Shara & Hurley (2002), who applied this to open clusters. They found that the supra-Chandrasekhar WD merger rate can be increased by an order of magnitude (although their statistics were based on only a few events). We did not find such an increase compared to the field population, where star formation is continuing, though we found some increase compared to the case without dynamical interactions (see Table 5). However, we note that our total number of supra-Chandrasekhar WD mergers is large. In fact, if indeed all those mergers lead to formation of NSs, and those NSs are retained by the cluster, then this channel provides about 6 per cent of all NSs ever created. The NSs thus created become comparable in numbers to the NSs that were born with natal kicks and retained. The production of NSs via this channel can be reduced by reducing the efficiency of the CE. In this case, more binaries will merge during the CE phase and less supra-Chandrasekhar mergers will occur. We found, however, that even the reduction of $\alpha_{CE}$ $\lambda$ to 0.1 led only to a moderate decrease in the 'current' (at about 10 Gyr) production rate of supra-Chandrasekhar mergers, while their total production is only a bit smaller (see different models for 47 Tuc in Table 5). In addition, the production of NSs via AIC is comparable to the production of NSs via merger-induced collapse, and therefore also appears to be a significant source of NSs in GCs. The question of how many NSs can be created via different channels in GCs is very important, and will be addressed in more detail in Paper II.

We estimate the contribution of SNe Ia produced in GCs to total galactic SN rates. Assuming that $\sim 3 \times 10^7$ $M_\odot$ is contained in galactic GCs ($\sim$150 galactic GCs), we find that the single-degenerate channel from GCs can provide at best 1 SN per $\sim 10^6$ yr per galaxy, and the contribution of GCs is only several times higher if the double-degenerate channel (supra-Chandrasekhar) also results in SNe. In spiral galaxies, the rate of SNe Ia is 0.04–0.1 per century per galaxy (Mannucci et al. 2005) and, therefore, the contribution of GCs is not important. However, GCs can play a larger role in elliptical galaxies, where star formation has ceased and the rate of SNe Ia provided by the field population at the age of several Gyr is smaller by several hundred times per unit mass (see also Table 5). In addition, in ellipticals the specific frequency of GCs per galaxy luminosity unit is significantly higher than in spirals (up to 8.6 compared to 0.5 in the Milky Way, see e.g. Kim & Fabbiano 2004), and the total mass of GCs in ellipticals can become as high as $\sim$0.5 per cent of the total galaxy mass. As a result, the total production rate of SNe Ia from GCs becomes comparable to the rate in the rest of the host galaxy. It has been shown that the observational SN Ia rate consists of two components – a prompt component that is proportional to the star formation rate, and an extended component that is proportional to the total stellar mass (Scannapieco & Bildsten 2005). This is consistent with the behaviour of the formation rates of both the single- and double-degenerate channels in GCs, which peak during the first Gyr of the cluster evolution and have a flat distribution at later times. We therefore propose that GCs can increase the theoretically predicted rates of SNe Ia in elliptical galaxies.

### 4.5 Coalescing compact binaries as *LISA* sources

AM CVn systems discussed in Section 4.3, as well as most double WD mergers discussed in Section 4.4 (with the exclusion of a small fraction of mergers that are results of physical collision during hard binary encounters) are coalescing binaries driven by gravitational radiation. Prior to their mergers, or before and during the MT, they can be detectable as GW sources by *Laser Interferometer Space Antenna* (*LISA*). Their detectability is significantly enhanced when their orbital periods become smaller than about 2000 s (Benacquista, Portegies Zwart & Rasio 2001; Stroeer, Vecchio & Nelemans 2005), so their signals can be distinguished from the background noise produced by Galactic binaries. As the positional accuracy of *LISA* will be much greater for binaries with such short periods, these sources can be associated with specific GCs in our Galaxy.

From our simulations, we find that at any given moment, a typical cluster of 200 000 $M_\odot$ will contain 10 *LISA* sources on average, and at least three *LISA* binaries at any given moment; during 1 Gyr a cluster forms 180 *LISA* systems. A massive cluster like 47 Tuc, with mass $\sim 10^6$ $M_\odot$, will have at least 10 *LISA* sources at any given moment, and 40 *LISA* binaries on average. At an age of 10 Gyr, such a cluster can produce as many as three to 15 NS–WD *LISA*

© 2006 The Authors. Journal compilation © 2006 RAS, MNRAS

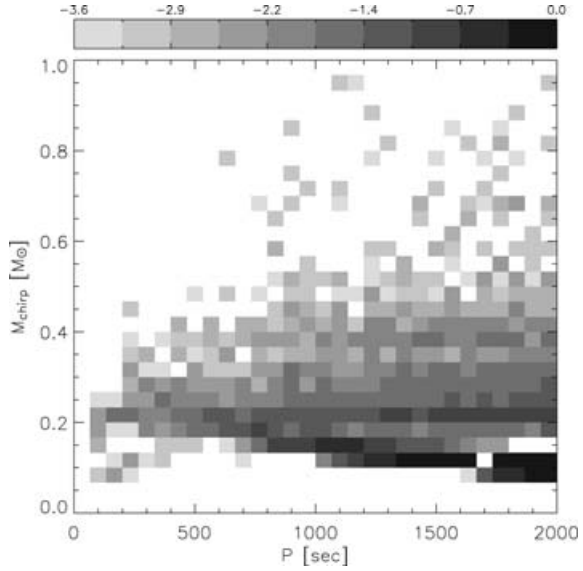


**Figure 18.** Distribution density (averaged over time) of *LISA* binaries, in the space of binary periods and chirp masses, from our 'standard' model (integrated over cluster ages from 9 to 13 Gyr).

binaries per Gyr (a typical cluster produces one to three NS–WD coalescing binaries per Gyr).

With the total mass in GCs of about $3 \times 10^7$ $M_\odot$, as many as 1500 *LISA* binaries can be present in all Galactic GCs (this number will decrease if the CE efficiency is smaller). The most optimistic upper limit for the galactic formation rate of NS–WD binaries in GCs is several hundred per Gyr. The lifetime of an NS–WD binary in the *LISA* band during the MT is $\sim 10^8$ yr. The time prior to the onset of MT depends on the binary eccentricity, but is usually much shorter (Ivanova et al. 2005c). With our predicted formation rates, as many as 10–50 NS–WD *LISA* binaries can be detected in GCs. This number is probably too optimistic, as fewer than 10 ultracompact X-ray binaries (mass-transferring NS–WD binaries with orbital periods less than an hour) have been identified in GCs, implying that the formation rate of *LISA* sources should be smaller. (One explanation could be that many GCs are less dense than our 'standard' model and NS–WD formation is thus less frequent.) We will address the issue of the formation rates of binaries with NSs in more detail in Paper II. Here, we will only note that the *LISA* binaries will spend most of their time in the *LISA* band among their MT tracks, with chirp masses $\lesssim 0.25$ $M_\odot$ (see Fig. 18). Our rates for WD–WD and NS–WD binaries differ from those in Benacquista (2006) (see also Davies 1995; Davies & Benz 1995). We predict about an order of magnitude more WD–WD *LISA* binaries, and our NS–WD *LISA* binary rates are at the lower end of the quoted range in Benacquista (2006).

## 5 DISCUSSION

With our simulations, we predict that the formation rates of CVs and AM CVn systems in GCs are not very different from those in the field population. The numbers of CVs and AM CVn systems per mass unit are comparable to numbers in the field if the whole cluster population is considered, and they are only two to three times larger in the core than in the field. Dynamical formation is responsible only for 60–70 per cent of CVs in the core. This fraction decreases as the density decreases, and the role of primordial CVs becomes more important. We rule out TCs as an effective mechanism for CV formation in GCs, unless the rate of TCs is significantly underestimated. Instead, we propose that the population of GC CVs reflects a combination of primordial CVs, CVs in post-exchange binaries, and products of physical collisions of MS stars with RGs. There are also primordial CVs which are located in the halo and have never entered the core. The GC core density variation indeed does not play a very large role, in contrast to the case of NS binaries, where almost all systems are formed dynamically (Ivanova et al. 2005c) and whose numbers have a strong dependence on the cluster collision rate (Pooley et al. 2003). We expect to have one detectable CV per 1000 $M_\odot$ in the core of a typical cluster and about one detectable CV per 1000–2000 $M_\odot$ in a 47 Tuc type cluster. Thus, we predict 35–40 CVs in the core of 47 Tuc, in quite reasonable agreement with observations, where 22 CVs in 47 Tuc have been identified (Edmonds et al. 2003a). Even better agreement between our simulations and the observed number of CVs can be obtained if we assume that the initial core mass in 47 Tuc is smaller than 5 per cent of the cluster.

Although the formation rates do not differ strongly, we found significant differences in the populations, and note that these differences may have observational consequences. Indeed, CVs in GCs have an unusual array of characteristics, which make them difficult to classify as members of the standard classes of CVs recognized in the Galaxy. Their X-ray luminosities seem to be rather high, compared with CVs in the field (Verbunt et al. 1997). They exhibit DNOs only rarely, compared to well-studied field dwarf novae: only 1 dwarf nova was found in 47 Tuc by Shara et al. (1996) in a survey which would have detected one-third of known dwarf novae if they were located in 47 Tuc, whereas Edmonds et al. (2003a) identified 22 firm CVs in 47 Tuc. Finally, the X-ray-to-optical flux ratios of CVs in GCs are relatively high, comparable to those of dwarf novae (Edmonds et al. 2003b).

One solution to this problem was the suggestion that CVs in GCs tend to be primarily magnetic in nature, compared to CVs in the field (Grindlay et al. 1995). Magnetic CVs have no discs (AM Her or polar CVs), or truncated discs [DQ Her CVs or intermediate polars (IPs)], because of the effect of the WD magnetic field. As a result, the disc instability is non-existent or suppressed. Magnetic CVs are believed to produce X-rays through an accretion shock above the polar cap, producing high X-ray luminosities, whereas non-magnetic CVs produce an optically thick boundary layer, saturating their X-ray emission (Patterson & Raymond 1985). Strong He II λ 4686 lines were observed in the spectra of three CVs in NGC 6397 (Edmonds et al. 1999), indicating a strong source of far-ultraviolet (FUV) radiation. This FUV radiation could indicate evidence either for an IP interpretation, or for a very high MT rate; the second interpretation is favoured for the FUV-bright, 27-h period CV AKO9 in 47 Tuc (Knigge et al. 2003). Another argument in favour of the IP interpretation is the excess $N_{\rm H}$ (in addition to that expected along the line of sight) observed towards many CVs in 47 Tuc (Heinke et al. 2005). Excess $N_{\rm H}$ in CVs that are not observed at high inclinations has been considered a signature of the accretion curtains observed in the magnetic systems known as IPs.

However, only two GC CVs have shown clear evidence of magnetic fields in their X-ray light curves so far (X9 and X10 in 47 Tuc Grindlay et al. 2001a; Heinke et al. 2005). This may not mean that these systems are not magnetic, since the number of X-ray photons detected from GCs is generally small (compared with nearby, well-studied CVs). In addition, it has been suggested that the accretion in SW Sex and VY Scl CVs is governed by the WD magnetic field, without evidence of pulsations (Rodríguez-Gil et al. 2001;

© 2006 The Authors. Journal compilation © 2006 RAS, MNRAS

Hameury & Lasota 2002). Another problem for the magnetic interpretation is that IPs tend to be optically brighter than typical CVs in GCs, which have lower ratios of X-ray to optical flux more typical of dwarf novae than IPs (Edmonds et al. 2003b). A final problem is the observation of DNOs in two of the three CVs in NGC 6397 possessing strong He II emission (Shara et al. 2005). A proposed resolution to these problems is a combination of a low MT rate (which will reduce the optical brightness and increase the X-ray-to-optical flux ratio) with an IP nature (Edmonds et al. 2003b). Dobrotka et al. (2006) calculated the dwarf nova recurrence times for CV discs with various MT rates and WD magnetic moments, and found a parameter space that fulfilled the requirements of GC CVs. Left unanswered was why GC CVs might tend to have stronger magnetic fields than field systems have.

Our work provides a possible answer to this question. GC dynamics has a strong effect on the composition of the binaries that form CVs, tending to place more-massive WDs into binaries that will become CVs (Fig. 11). Increasing the mass of WDs in CVs increases the energy that can be extracted at a given MT rate, thus increasing the X-ray luminosity and X-ray-to-optical flux ratio of the CVs. This effect is complementary to the effects of higher magnetic fields. However, higher-mass WDs also have a higher probability of showing strong magnetic fields (Vennes 1999; Liebert, Bergeron & Holberg 2003; Wickramasinghe & Ferrario 2005). Thus, the dynamical origin of WDs in GC CVs may be responsible for the observational peculiarities of GC CVs, their relatively high X-ray luminosities and X-ray to optical flux ratios, and their low rates of DNOs.

The tendency for higher-mass WD accretors in GC CVs in comparison to the field also affects the production of the superhump phenomenon. This behaviour results from the precession of the outer disc due to the excitation of resonances within the disc caused by the 3:1 commensurability of motions in the disc with the companion's orbital period (see Whitehurst & King 1991). Such systems are characterized by mass ratios (of donor to accretor) of less than 0.25–0.33. Systems of this type in the field are rarely observed at orbital periods above the period gap, but the higher WD masses of CVs in GCs would increase their likelihood in GCs.

We examined also several other consequences of having a dynamically modified population of close binaries including WDs. In particular, considering supra-Chandrasekhar mergers, we found that NSs may be overproduced if these mergers lead to merger-induced collapse. We suggest that either this mechanism does not lead to NS formation, or the CE efficiency is overestimated. By our estimates, GCs do not contribute strongly to the SN Ia rates in spiral galaxies; however, they may significantly increase these rates in elliptical galaxies. We have also shown that GCs can be excellent targets for *LISA* observations since many GCs will contain several *LISA* sources at any given moment, although most of those systems will have low chirp masses.

## ACKNOWLEDGMENTS

This work was supported in part by NASA Grants NAG5-12044 and NNG04G176G (FAR), NSF Grant AST-0200876 (RET), *Chandra* Theory Grant TM6-7007X (JF), and the Lindheimer Fellowship (COH) at Northwestern University. KB acknowledges support from KBN Grant 1P03D02228. All simulations were performed on the McKenzie cluster at CITA, which was funded by the Canada Foundation for Innovation and the Ontario Innovation Trust (Dubinski et al. 2003).

## REFERENCES

Bailyn C. D., Grindlay J. E., Garcia M. R., 1990, ApJ, 357, L35
Bailyn C. D., Rubenstein E. P., Slavin S. D., Cohn H., Lugger P., Cool A. M., Grindlay J. E., 1996, ApJ, 473, L31
Bassa C. et al., 2004, ApJ, 609, 755
Belczynski K., Kalogera V., Bulik T., 2002, ApJ, 572, 407
Belczynski K., Benacquista M., Larson S. L., Ruiter A. J., 2005a, preprint (astro-ph/0510718)
Belczynski K., Bulik T., Ruiter A. J., 2005b, ApJ, 629, 915
Belczynski K., Kalogera V., Rasio F. A., Taam R. E., Zezas A., Bulik T., Maccarone T. J., Ivanova N., 2005c, preprint (astro-ph/0511811)
Benacquista M. J., 2006, Living Reviews in Relativity, 9, 2
Benacquista M. J., Portegies Zwart S., Rasio F. A., 2001, Class. Quantum Gravity, 18, 4025
Chen K., Leonard P. J. T., 1993, ApJ, 411, L75
Clark G. W., 1975, ApJ, 199, L143
Cool A. M., Grindlay J. E., Cohn H. N., Lugger P. M., Slavin S. D., 1995, ApJ, 439, 695
Cool A. M., Grindlay J. E., Cohn H. N., Lugger P. M., Bailyn C. D., 1998, ApJ, 508, L75
Davies M. B., 1995, MNRAS, 276, 887
Davies M. B., 1997, MNRAS, 288, 117
Davies M. B., Benz W., 1995, MNRAS, 276, 876
Davies M. B., Benz W., Hills J. G., 1991, ApJ, 381, 449
Di Stefano R., Rappaport S., 1994, ApJ, 423, 274
Dobrotka A., Lasota J.-P., Menou K., 2006, ApJ, 640, 288
Dubinski J., Humble R. J., Loken C., Pen U.-L., Martin P., 2003, Proc. 17th Annual International Symp., High Performance Computing Systems and Applications
Edmonds P. D., Grindlay J. E., Cool A., Cohn H., Lugger P., Bailyn C., 1999, ApJ, 516, 250
Edmonds P. D., Gilliland R. L., Heinke C. O., Grindlay J. E., 2003a, ApJ, 596, 1177
Edmonds P. D., Gilliland R. L., Heinke C. O., Grindlay J. E., 2003b, ApJ, 596, 1197
Fregeau J. M., Cheung P., Portegies Zwart S. F., Rasio F. A., 2004, MNRAS, 352, 1
García-Senz D., Bravo E., Woosley S. E., 1999, A&A, 349, 177
Grindlay J. E., Cool A. M., Callanan P. J., Bailyn C. D., Cohn H. N., Lugger P. M., 1995, ApJ, 455, L47
Grindlay J. E., Heinke C., Edmonds P. D., Murray S. S., 2001a, Sci, 292, 2290
Grindlay J. E., Heinke C. O., Edmonds P. D., Murray S. S., Cool A. M., 2001b, ApJ, 563, L53
Hakala P. J., Charles P. A., Johnston H. M., Verbunt F., 1997, MNRAS, 285, 693
Hameury J.-M., Lasota J.-P., 2002, A&A, 394, 231
Hannikainen D. C., Charles P. A., van Zyl L., Kong A. K. H., Homer L., Hakala P., Naylor T., Davies M. B., 2005, MNRAS, 357, 325
Hansen B. M. S., Kalogera V., Rasio F. A., 2003, ApJ, 586, 1364
Heggie D. C., Hut P., McMillan S. L. W., 1996, ApJ, 467, 359
Heinke C. O., Grindlay J. E., Lugger P. M., Cohn H. N., Edmonds P. D., Lloyd D. A., Cool A. M., 2003, ApJ, 598, 501
Heinke C. O., Grindlay J. E., Edmonds P. D., Cohn H. N., Lugger P. M., Camilo F., Bogdanov S., Freire P. C., 2005, ApJ, 625, 796
Hurley J. R., Tout C. A., Pols O. R., 2002, MNRAS, 329, 897
Ivanova N., 2006, ApJ, 636, 979
Ivanova N., Rasio F., 2004, in Tovmassian G., Sion E., eds, Rev. Mex. Astron. Astrofis. Ser. Conf. Vol. 20, Compact Binaries in the Galaxy and Beyond. UNAM, Mexico, p. 67
Ivanova N., Taam R. E., 2003, ApJ, 599, 516 (IT03)
Ivanova N., Taam R. E., 2004, ApJ, 601, 1058
Ivanova N., Rasio F. A., 2005, in Burderi L., Antonelli L. A., D'Antona F., di Salvo T., Israel G. L., Piersanti L., Tornambè A., Straniero O., eds, AIP Conf. Proc. 797, Interacting Binaries: Accretion, Evolution, and Outcomes. Am. Inst. Phys., New York, p. 53

© 2006 The Authors. Journal compilation © 2006 RAS, MNRAS

Ivanova N., Belczynski K., Fregeau J. M., Rasio F. A., 2005a, MNRAS, 358, 572
Ivanova N., Fregeau J. M., Rasio F. A., 2005b, in Rasio F. A., Stairs I. H., eds, ASP Conf. Ser. Vol. 328, Binary Radio Pulsars Binary Evolution and Neutron Stars in Globular Clusters. Astron. Soc. Pac., San Francisco, p. 231
Ivanova N., Rasio F. A., Lombardi J. C., Dooley K. L., Proulx Z. F., 2005c, ApJ, 621, L109
Kaluzny J., Thompson I. B., 2003, AJ, 125, 2534
Kaluzny J., Pietrukowicz P., Thompson I. B., Krzeminski W., Schwarzenberg-Czerny A., Pych W., Stachowski G., 2005, MNRAS, 359, 677
Kato M., Hachisu I., 1999, ApJ, 513, L41
Kim D.-W., Fabbiano G., 2004, ApJ, 611, 846
Knigge C., Zurek D. R., Shara M. M., Long K. S., Gilliland R. L., 2003, ApJ, 599, 1320
Kroupa P., 2002, Science, 295, 82
Leibundgut B., 2001, ARA&A, 39, 67
Levan A. J., Wynn G. A., Chapman R., Davies M. B., King A. R., Priddey R. S., Tanvir N. R., 2006, MNRAS, 368, L1
Liebert J., Bergeron P., Holberg J. B., 2003, AJ, 125, 348
Livne E., Glasner A. S., 1991, ApJ, 370, 272
Lombardi J. C., Proulx Z. F., Dooley K. L., Theriault E. M., Ivanova N., Rasio F. A., 2006, ApJ, 640, 441
Mannucci F., Della Valle M., Panagia N., Cappellaro E., Cresci G., Maiolino R., Petrosian A., Turatto M., 2005, A&A, 433, 807
Mardling R. A., 1995, ApJ, 450, 732
Neill J. D., Shara M. M., Caulet A., Buckley D. A. H., 2002, AJ, 123, 3298
Nelemans G., Portegies Zwart S. F., Verbunt F., Yungelson L. R., 2001, A&A, 368, 939
Patterson J., Raymond J. C., 1985, ApJ, 292, 535
Pfahl E., Rappaport S., Podsiadlowski P., 2002, ApJ, 573, 283
Podsiadlowski P., Langer N., Poelarends A. J. T., Rappaport S., Heger A., Pfahl E., 2004, ApJ, 612, 1044
Pietrukowicz P., Kaluzny J., Thompson I. B., Jaroszynski M., Schwarzenberg-Czerny A., Krzeminski W., Pych W., 2005, Acta Astron., 55, 261
Pooley D., Hut P., 2006, ApJ, 646, L143
Pooley D. et al., 2002, BAAS, 34, 1313
Pooley D. et al., 2003, ApJ, 591, L131
Portegies Zwart S. F., Meinen A. T., 1993, A&A, 280, 174
Rappaport S., Verbunt F., Joss P. C., 1983, ApJ, 275, 713 (RVJ)
Rasio F. A., Shapiro S. L., 1991, ApJ, 377, 559
Rodríguez-Gil P., Casares J., Martínez-Pais I. G., Hakala P., Steeghs D., 2001, ApJ, 548, L49
Scannapieco E., Bildsten L., 2005, ApJ, 629, L85
Shara M. M., Drissen L., 1995, ApJ, 448, 203
Shara M. M., Hurley J. R., 2002, ApJ, 571, 830
Shara M. M., Bergeron L. E., Gilliland R. L., Saha A., Petro L., 1996, ApJ, 471, 804
Shara M. M., Hinkley S., Zurek D. R., Knigge C., Dieball A., 2005, AJ, 130, 1829
Stroeer A., Vecchio A., Nelemans G., 2005, ApJ, 633, L33
Taam R. E., 1980, ApJ, 242, 749
Vennes S., 1999, ApJ, 525, 995
Verbunt F., Bunk W. H., Ritter H., Pfeffermann E., 1997, A&A, 327, 602
Whitehurst R., King A., 1991, MNRAS, 249, 25
Wickramasinghe D. T., Ferrario L., 2005, MNRAS, 356, 1576
Woosley S. E., Weaver T. A., 1994, ApJ, 423, 371

This paper has been typeset from a TEX/LATEX file prepared by the author.

© 2006 The Authors. Journal compilation © 2006 RAS, MNRAS